Available online at www.sciencedirect.com

SciVerse ScienceDirect

Neuromuscular Disorders 23 (2013) 84–88

www.elsevier.com/locate/nmd

Respiratory dysfunction in patients severely affected by GNE myopathy (distal myopathy with rimmed vacuoles)

Madoka Mori-Yoshimura [a,*], Yasushi Oya [a], Yukiko K. Hayashi [b,c], Satoru Noguchi [b], Ichizo Nishino [b,c], Miho Murata [a]

[a] *Department of Neurology, National Center Hospital, National Center of Neurology and Psychiatry, 4-1-1 Ogawahigashi, Kodaira, Tokyo 187-8551, Japan*

[b] *Department of Neuromuscular Research, National Institute of Neuroscience, National Center of Neurology and Psychiatry, 4-1-1 Ogawahigashi, Kodaira, Tokyo 187-8502, Japan*

[c] *Translational Medical Center, National Center of Neurology and Psychiatry, 4-1-1 Ogawahigashi, Kodaira, Tokyo 187-8502, Japan*

Received 28 March 2012; received in revised form 23 July 2012; accepted 25 September 2012

Abstract

GNE myopathy is a rare and mildly progressive autosomal recessive myopathy caused by *GNE* mutations. Respiratory dysfunction has not been reported in GNE myopathy patients. In this study, we retrospectively reviewed the respiratory function of 39 severely affected GNE myopathy patients (13 men, 26 women) from medical records, and compared these parameters with various other patient characteristics (e.g., *GNE* mutations, age at onset, creatine kinase levels, and being wheelchair-bound) for correlations. The mean % forced vital capacity [FVC] was 92 (26) (range, 16–128). In 12/39 (31%) patients, %FVC was <80%. Of these 12 patients, 11 (92%) were entirely wheelchair-dependent. These patients exhibited significantly earlier onset (20 [4] vs. 30 [8] years, $p < 0.001$) and lower creatine kinase levels (56 [71] vs. 279 [185] IU/L) than patients with normal respiratory function. Two patients exhibited severe respiratory failure and required non-invasive positive pressure ventilation. Patients with a homozygous mutation in the *N*-acetylmannosamine kinase domain exhibited lower %FVC; while only one compound heterozygous patient with separate mutations in the uridinediphosphate-*N*-acetylglucosamine 2-epimerase and the *N*-acetylmannosamine kinase domains had respiratory dysfunction. Our results collectively suggest that GNE myopathy can cause severe respiratory failure. Respiratory dysfunction should be carefully monitored in patients with advanced GNE myopathy characterized by early onset and homozygous homozygous mutations in the *N*-acetylmannosamine kinase domain.

Keywords: GNE myopathy; Distal myopathy with rimmed vacuoles (DMRV); Hereditary inclusion body myopathy; Respiratory dysfunction; Uridinediphosphate-*N*-acetylglucosamine (UDP-GlcNAc) 2-epimerase domain; *N*-acetylmannosamine kinase domain

1. Introduction

GNE myopathy, also known as distal myopathy with rimmed vacuoles (DMRV), Nonaka myopathy, or hereditary inclusion body myopathy (hIBM), is an early adult-onset, slowly progressive myopathy that preferentially affects the tibialis anterior muscle but relatively spares the quadriceps femoris muscles [1,2]. Respiratory dysfunction has not been reported in GNE myopathy [3]. Nonaka et al. reported that respiratory muscles were rarely involved even in bed-ridden patients, but no data were presented [1]. However, we had noticed that a few patients with GNE myopathy exhibited mild but progressive respiratory loss, with some experiencing recurrent pneumonia due to reduced airway clearance. Recent recommendations suggest training patients with neuromuscular disease with respiratory dysfunction using the air stacking technique to increase their thorax capacity and assisted cough peak flow (CPF) from an early stage to maintain lung compliance and chest mobility, and to clean the airways [4]. If respiratory dysfunction is not rare in patients with GNE

* Corresponding author. Tel.: +81 341 2711; fax: +81 342 1852.
E-mail address: yoshimur@ncnp.go.jp (M. Mori-Yoshimura).

0960-8966/$ - see front matter © 2012 Elsevier B.V. All rights reserved.
http://dx.doi.org/10.1016/j.nmd.2012.09.007

myopathy, then, physicians should punctually monitor their respiratory function with pulmonary function tests to look for early signs of respiratory dysfunction, perform respiratory training, coup with airway infection using a mechanical in-exsufflator (MI-E), and induce mechanical ventilation if required, as they do for patients with neuromuscular disease who exhibit respiratory failure.

The aim of this study is to evaluate past and present clinical respiratory function test parameters of GNE myopathy patients, and analyze factors that correlate with disease severity.

2. Patients and methods

2.1. Study population

Medical records of all genetically confirmed GNE myopathy patients who underwent pulmonary function tests at the National Center Hospital, National Center of Neurology and Psychiatry, were retrospectively reviewed. We collected data on genetic diagnosis, respiratory function (% vital capacity [%VC], % force vital capacity [FVC], cough peak flow [CPF]), creatine kinase (CK), chest X-ray and/or CT scan and body mass index (BMI) for analysis.

2.2. Data handling and analysis

Data were summarized using descriptive statistics, and each variable was compared against age, sex, respiratory dysfunction (whether their %FVC was up to or over 80%), and domain mutation (i.e., within the UDP-GlcNAc 2-epimerase domain: ED or *N*-acetylmannosamine kinase domain: KD). The *t*-test was used to compare the means of each group. Data for the two study populations were calculated using chi-square contingency table analysis. Multivariate regression analysis was performed with %FVC as the dependent variable. Explanatory variables included age at disease onset, CK and BMI. We found that the variables age, duration from onset to present, age upon wheelchair use, age at loss of ambulation, were highly correlated (over 0.5) with age at disease onset. As such, we eliminated these three due to multicolinearity in the multivariate regression analysis. When past %FVC data were available, the present data were compared with serial changes in respiratory function during the preceding 5–7 years, and changes in %FVC over time were determined by calculating the difference between past and present data. All analyses were performed using SPSS for Macintosh (Version 18; SPSS Inc., Chicago, IL).

3. Results

3.1. General characteristics

A total of 39 Japanese patients (13 men, 26 women) were recruited. The mean age at the time of data collection was 43.1 (11.3) years (mean [standard deviation, SD]) (Table 1). The mean age at first appearance of symptoms was 26.8 (9.0) years (range, 15–58 years; median, 25 years). Present age, age at disease onset, age at wheelchair use, and present ambulation status were not significantly different between men and women; 20.5% (8/39) had symptom onset before age 20. Of the 39 patients, 51.3% (20/39) could walk but needed assistance, and 69.2% (27/39) were wheelchair-bound (8/27 and 19/27 were partially and totally wheelchair-bound, respectively). Age at first use of a wheelchair was 33.3 (10.8) years (range, 18–59 years; median, 31.5 years) and that for loss of ambulation was 36.9 (11.9) years (Table 1).

3.2. GNE mutations

Of the 39 patients, 30.7% (12/39) carried homozygous mutations, while 69.2% (27/39) harbored compound heterozygous mutations (Supplementary Table 1). Among the homozygous patients, 66.7% (8/12) harbored the p.V572L mutation. Among the compound heterozygous patients, 25.9% (7/27) exhibited the p.D176V/p.V572L genotype, while the other patients each had a different mutation. With respect to the location of the mutation (i.e., protein domain), 28.2% (11/39) homozygous patients carried mutations only in ED (ED/ED), 46.2% patients (18/39) were compound heterozygotes with 1 mutation each in the ED and KD (ED/KD), and 25.6% patients (10/39) had a mutation in the KD of both genes (KD/KD) (Table 2). The allelic frequencies of p.V572L, p.D165V, p.C13S, and p.R129Q were 35.9% (28/78), 28.2% (22/78), 11.5% (9/78), and 2.6% (2/78), respectively, while all other mutations had only 1 allele each (Supplementary Table 1).

3.3. Respiratory function

None of the patients had lung and/or thoracic diseases that could affect their respiratory function in chest X-ray and/or chest computed tomography. The %VC and %FVC in patients with GNE myopathy were 91.9 (26.9) (range, 18.2–126.3; median, 100.3) and 92.0 (25.8) (range, 16.4–128.5; median, 100.5; Table 1), respectively.

3.4. Patients with respiratory dysfunction

In 30.7% of patients (12/39), %FVC was <80. Of these 12 patients, 91.6% (11/12) were wheelchair-dependent and 83.3% (10/12) had already lost ambulation. Their onset was significantly earlier (19.3 [4.4] vs. 30.3 [8.4], $p < 0.001$) and mean CK level was significantly lower (55.8 [71.6] vs. 279.0 [184.7], $p = 0.004$) than those of patients with normal respiratory function. Four patients exhibited advanced respiratory dysfunction (%FVC < 50% and cough peak flow [CPF] < 160 L/min) (Table 2). All 4 patients had experienced recurrent pneumonia, and 2 patients required nocturnal NPPV. They were all early onset (before 20 years old) and non-ambu-

Table 1
Patient characteristics by respiratory function.

	Total	%FVC ⩾ 80%	%FVC < 80%	
n	*39*	27	12	*p*
Age (years)	43.0 ± 11.3	44.3 ± 11.7	39.9 ± 10.3	0.267
Age at onset (years)	26.8 ± 9.0	30.2 ± 8.4	19.2 ± 4.4	<0.001
GNE/GNE	10 (25.6%)	7 (70.0%)	3 (30.0%)	0.640
GNE/MNK	18 (46.2%)	16 (88.9%)	2 (11.1%)	0.018
MNK/MNK	11 (28.2%)	4 (36.4%)	7 (63.6%)	0.009
Duration from onset of disease to present	16.2 ± 8.4	14.1 ± 7.8	20.8 ± 8.2	0.021
Wheelchair use (%)	27 (69.2%)	16 (59.3%)	11 (40.7%)	0.141
Wheelchair use since (years)	33.3 ± 10.8	37.9 ± 11.3	26.6 ± 5.1	0.002
Lost ambulation	19 (48.7%)	8 (42.1%)	11 (57.9%)	0.014
Age at lost ambulation (years)	36.9 ± 11.9	41.2 ± 11.7	28.2 ± 6.4	0.018
CK (IU/L)	201.3 ± 187.5	279.0 ± 184.7	55.8 ± 71.6	0.004
BMI	21.1 ± 4.2	20.8 ± 3.2	21.9 ± 5.8	0.457
FVC (%)	91.9 ± 26.9	106.9 ± 12.5	58.2 ± 18.7	<0.001
VC (%)	92.0 ± 25.8	106.4 ± 11.6	59.5 ± 17.6	<0.001
CPF (L/min)	334.2 ± 139.5	378.0 ± 105.7	250.2 ± 161.5	0.008

Most patients with reduced respiratory function had already lost ambulation and were entirely wheelchair-dependent. Their onset was significantly earlier and CK levels significantly lower than those of patients with normal respiratory function. FVC: forced vital capacity, VC: vital capacity, CPF: cough peak flow, BMI: body mass index, CK: creatine kinase.

Table 2
Patients with FVC < 50% and CPF < 160 L/min.

Case	Age	Sex	Mutation	Mutant domain	Ambulation status	Disease onset	Disease duration	Age at lost ambulation	%VC	%FVC	CPF (L/min)	Reccurent pneumonea	NPPV	CK (IU/L)	BMI
1	51	Man	p.C13S homozygote	ED/ED	Non-ambulant	17	34	25	18.2	16.4	48.0	Yes	Nocturnal	13	18.6
2	42	Woman	p.V572L homozygote	KD/KD	Non-ambulant	16	26	23	37.6	34.4	141.6	Yes	Nocturnal	13	22.2
3	45	Woman	p.V572L homozygote	KD/KD	Non-ambulant	17	28	31	49.0	48.3	147.6	Yes	No	8	31.6
4	37	Woman	p.V572L homozygote	KD/KD	Non-ambulant	16	21	24	53.7	48.6	118.8	Yes	No	No data	20.4

Table 3
Multivariate regression analysis of predictive factors for respiratory dysfunction.

	Regression coefficient	*p*	Lower limit of 95% confidence interval	Upper limit of 95% CI
Age at onset	0.949	0.042	0.038	1.86
CK	0.068	0.008	0.02	0.115
BMI	−1.8	0.09	−3.811	0.302

Multivariate linear regression analysis was performed to evaluate the relationship between %FVC and other clinical parameters. Age at onset and CK were significantly correlated with %FVC.

lant. The majority (7/12) of patients had KD/KD mutations, whereas significantly fewer patients with respiratory dysfunction had ED/KD mutations.

In order to identify predictive factors for respiratory dysfunction in GNE myopathy, we performed multivariate analysis to determine the relationship with %FVC. This revealed age at onset ($p = 0.042$) and CK ($p = 0.008$) as significantly correlated to %FVC (Table 3, Fig. 1).

Past (5–7 years ago) data were available for 9 patients. The %FVC decrements in 5 patients with respiratory dysfunction were significantly greater than those of patients without dysfunction (20.9 [6.0] vs. 0.8 [9.7], $p = 0.004$; Supplementary Table 2).

4. Discussion

To our knowledge, we are the first to report respiratory dysfunction in GNE myopathy. Our study demonstrates that (1) certain GNE myopathy patients in Japan exhibit respiratory dysfunction, and (2) early onset and lower CK levels resulting from severe muscle atrophy and weakness, and KD/KD mutations can be risk factors for respiratory dysfunction.

Malicdan et al. reported that pathological changes in the diaphragms of the GNE (−/−) hGNED176V-Tg model mice were variable and ranged from almost normal to the presence of marked fibrosis and rimmed vacuoles. On the other hand, the gastrocnemius muscles of all mice exhibited myopathic features [5]. The features in these mice correspond to individual differences observed in the patients of our study. The fact that not all cases in our study exhibited respiratory dysfunction as observed in the GNE (−/−)

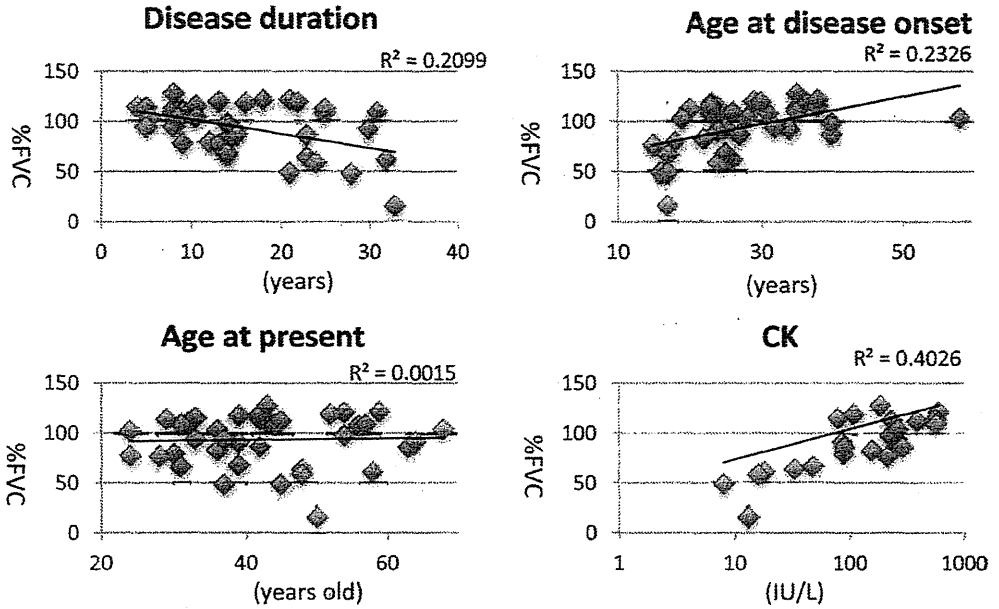

Fig. 1. Scatterplots of %FVC as functions of age, age at disease onset, disease duration, and creatine kinase (CK) level. Age at disease onset, disease duration, and CK level were correlated with %FVC.

hGNED176V-Tg mice indicates that severe respiratory muscle involvement is not a constant feature of GNE myopathy. Yet, since about 30% of patients had decreased %FVC and severe respiratory dysfunction was overlooked by neurologists or physicians, clinicians should be made more aware of the possibility of respiratory dysfunction, particularly in patients with advanced GNE myopathy. If %VC decreases to 70%, patients should be taught air stacking as with other neuromuscular disorders [4,6]. CPF should be routinely measured in patients with GNE myopathy, given that its decrement was associated with recurrent pneumonia in our study. Early induction of assisted CPF and/or MI-E is required if patients with reduced CPF have an airway infection. Serial data suggest that %FVC decreased from the normal range to %FVC < 80, indicating that continuous monitoring is required even in patients with normal respiratory function. Moreover, respiratory function parameters may provide quantitatively useful data for clinical trials, particularly those directed to non-ambulant patients.

All 4 patients with severe respiratory dysfunction exhibited early onset, homozygous mutations, and advanced muscle weakness. However, not all early onset, homozygous, or non-ambulant patients exhibited severe respiratory dysfunction. Although the underlying reasons are unclear, we also found that ED/KD mutations were less associated with decreased respiratory function, while many patients with KD/KD mutations showed respiratory dysfunction. A large scale, cross-sectional study could better identify key factors responsible for respiratory dysfunction and genotype-phenotype correlations.

We are aware that the recruitment of patients from NCNP, highly specialized for muscle disease, is a potential source of selection bias, because they may be particularly more severely affected than the general patient population. Therefore, our study may not correctly reflect the general patient population. Investigations of small populations may underestimate the statistical significance as well. However, our previous GNE myopathy questionnaire study revealed a similar correlation between genotypes and phenotypes [7]. We are currently in the process of establishing a Japanese national GNE myopathy patient registry called Registration of Muscular Dystrophy (REMUDY, http://www.remudy.jp) to perform a broader epidemic investigation of associated conditions, including respiratory dysfunction. To clarify the relationship between respiratory dysfunction and other clinical/laboratory factors, we have initiated a prospective observational study on GNE myopathy.

Three of 4 patients with severe respiratory dysfunction had homozygous p.V572L mutations. Given the frequency of the p.V572L mutation in the Japanese population, it will be interesting to determine whether non-Japanese individuals harboring this mutation also exhibit respiratory dysfunction.

In conclusion, advanced GNE myopathy patients are at risk for respiratory dysfunction. The KD/KD genotype, early onset, loss of ambulation/wheelchair use, and low CK level resulted in advanced muscle atrophy may be associated with respiratory dysfunction.

Acknowledgments

We thank members of the Patients Association for Distal Myopathies in Japan (PADM). This work was partly supported by Research on Intractable Diseases of Health

and Labour Sciences Research Grants, Comprehensive Research on Disability Health and Welfare Grants, Health and Labour Science Research Grants, Intramural Research Grant (23-5/23-4) for Neurological and Psychiatric Disorders from the NCNP, and Young Investigator Fellowship from the Translational Medical Center, National Center of Neurology and Psychiatry.

Appendix A. Supplementary data

Supplementary data associated with this article can be found, in the online version, at http://dx.doi.org/10.1016/j.nmd.2012.09.007.

References

[1] Nonaka I, Sunohara N, Satoyoshi E, Terasawa K, Yonemoto K. Autosomal recessive distal muscular dystrophy: a comparative study with distal myopathy with rimmed vacuole formation. Ann Neurol 1985;17:51–9.

[2] Argov Z, Yarom R. "Rimmed vacuole myopathy" sparing the quadriceps. A unique disorder in Iranian Jews. J Neurol Sci 1984;64:33–43.

[3] Udd B, Griggs RC. Nonaka myopathy. In: Engel AG, Franzini-Armstrong C, editors. Myology. New York: McGraw-Hill; 2004. p. 1178–9.

[4] Bach JR. Noninvasive respiratory muscle aids. In: Bach JR, editor. Management of patients with neuromuscular disorders. Philadelphia: Hanley & Belfus; 2004. p. 211–69.

[5] Malicdan MC, Noguchi S, Nonaka I, Hayashi YK, Nishino I. A Gne knockout mouse expressing human GNE D176V mutation develops features similar to distal myopathy with rimmed vacuoles or hereditary inclusion body myopathy. Hum Mol Genet 2007;16:2669–82.

[6] Bach JR. Pulmonary defense mechanisms and cough peak flow. In: Bach JR, editor. Management of patients with neuromuscular disorders. Philadelphia: Hanley & Belfus; 2004. p. 193–9.

[7] Mori-Yoshimura M, Monma K, Suzuki N, et al. GNE myopathy (distal myopathy with rimmed vacuoles) patients with mutations in the UDP-GlcNAc 2-epimerase and in the *N*-acetylmannosamine kinase domains of the GNE gene exhibit less severe phenotypes than patients with mutations only in MNK domain. J Neurol Sci, 2012. [Epub ahead of print].

Clinical Neurology and Neurosurgery 114 (2012) 678–683

Contents lists available at SciVerse ScienceDirect

Clinical Neurology and Neurosurgery

journal homepage: www.elsevier.com/locate/clineuro

Case series

Clinicopathological features of centronuclear myopathy in Japanese populations harboring mutations in dynamin 2

Madoka Mori-Yoshimura[a], Aya Okuma[b], Yasushi Oya[a], Chieko Fujimura-Kiyono[c], Hideto Nakajima[c], Keita Matsuura[d], Aya Takemura[a], May Christine V. Malicdan[b], Yukiko K. Hayashi[b], Ikuya Nonaka[b], Miho Murata[a], Ichizo Nishino[b,*]

[a] Department of Neurology, National Center Hospital of Neurology and Psychiatry, 4-1-1 Ogawahigashi-cho, Kodaira, Tokyo 187-8551, Japan
[b] Department of Neuromuscular Research, National Institute of Neuroscience, National Center of Neurology and Psychiatry, 4-1-1 Ogawahigashi-cho, Kodaira, Tokyo 187-8502, Japan
[c] Department of Neurology, Osaka Medical College, Daigaku-Machi 2-7, Takatsuki, Osaka 569-8686, Japan
[d] Department of Neurology, Kinan Hospital 4750, Atawa, Mihama-chou, Minamimuro-gun, Mie 513-8505, Japan

ARTICLE INFO

Article history:
Received 25 October 2010
Received in revised form 26 October 2011
Accepted 30 October 2011
Available online 19 May 2012

Keywords:
Centronuclear myopathy
Dynamin 2
Congenital myopathy
Radial distribution
Clinicopathological homology

ABSTRACT

Background: Missense mutations in dynamin 2 gene (*DNM2*) are associated with autosomal dominant centronuclear myopathy (CNM) with characteristic histopathological findings of centrally located myonuclei in a large number of muscle fibers.
Methods: To identify Japanese CNM caused by *DNM2* mutations (DNM2-CNM), we sequenced *DNM2* in 22 unrelated Japanese patients who were pathologically diagnosed with CNM. The clinical and pathological findings of DNM2-CNM in patients were reviewed.
Results: We identified 3 different heterozygous missense mutations (p.E368K, p.R369W, and p.R465W) in 4 probands from 4 families. Clinically, calf muscle atrophy and *pes cavus* are features that are highly suggestive of DNM2-CNM among all CNMs. Pathologically, all 4 DNM2-CNM patients showed a radial distribution of myofibrils in scattered fibers, type 1 fiber atrophy, type 1 fiber predominance, and type 2C fibers. None of the non-DNM2-CNM patients exhibited all the 4 abovementioned pathological features, although some patients showed radial distribution without type 1 fiber atrophy and/or type 2C fibers.
Discussion: These results indicate that the clinicopathological features of DNM2-CNM are rather homogeneous and can be distinguished from the features of non-DNM2-CNM.

1. Introduction

Centronuclear myopathy (CNM) is a rare congenital myopathy named after its characteristic feature of centrally located nuclei in majority of the muscle fibers [1]. In autosomal dominant (AD) cases, muscular weakness and atrophy often begin in childhood or early adolescence [2,3]. CNM progresses slowly, and patients usually follow a mild course and can often expect a normal life-span. In muscle biopsy, a radial alignment of intermyofibrillar networks [1] is seen in nicotinamide adenosine dinucleotide-tetrazolium reductase (NADH-TR) preparations due to the presence of central nuclei; type 1 fiber atrophy is also often observed. Several families with CNM are found in Europe, the United States, Central Africa, Argentina, and Japan [2–6].

Thus far, 4 causative genes have been reported for CNM: myotubularin (*MTM1*), dynamin 2 (*DNM2*) [7], *hJUMPY* [8], and amphiphysin 2 (*BIN1*) [9]. Among them, *DNM2* mutations have been identified among patients in France, French Guiana, the United States, Belgium, Germany, Great Britain, Argentina, and Central Africa [6,10,11]. *DNM2* encodes a protein involved in endocytosis, membrane trafficking, actin assembly, and centrosome cohesion [12–14]. Thus, *DNM2* mutations cause a reduction of dynamin in transfected fibroblasts, leading to defects in centrosomal function.

Patients with CNM that is caused by mutation in the middle domain of *DNM2* (DNM2-CNM) present with a homogenous mild phenotype characterized by slowly progressing muscle weakness without cardiac or respiratory involvement [10]. Muscle computed tomography (CT) and MRI studies clearly show a relatively diffuse involvement in lower-leg muscles, while a selective pattern appears in thigh muscles [10,15,16]. Subtle mental impairment or peripheral nerve involvement was described in a previous report [17]. Mutations in the PH domain lead to an intermediate phenotype with mild respiratory failure and relatively severe weakness as compared to DNM2-CNM caused by middle-domain mutations [6]. Another study reported a more severe infantile form with hypotonia, weak suckling, and respiratory failure due to mutation in the PH domain of *DNM2* [11]. Although no *DNM2* mutations have

* Corresponding author. Tel.: +81 423461712; fax: +81 423461742.
E-mail address: nishino@ncnp.go.jp (I. Nishino).

0303-8467/$ – see front matter © 2011 Elsevier B.V. All rights reserved.
doi:10.1016/j.clineuro.2011.10.040

been identified among Japanese patients, there have been reports of patients with evidently similar clinicopathological features [4,5], suggesting the possibility of the presence of DNM2-CNM in the Japanese population. We therefore aimed at detecting *DNM2* mutations among Japanese CNM patients.

2. Materials and methods

2.1. Patients

We retrospectively recruited patients who were diagnosed with CNM or myotubular myopathy at the National Center of Neurology and Psychiatry and analyzed their samples from a total of 9639 muscle biopsies obtained between 1978 and 2006. Inclusion criteria were the presence of more than 6% centrally nucleated fibers and the absence of characteristic findings indicating other muscle diseases upon muscle biopsy. Our cohort consists of 22 unrelated patients aged 1–72 years: 2 had an AD family history; 5 had affected siblings, and consanguinity was documented in one of the patient's families; and 8 were sporadic cases. No record of family history was available for 7 patients. Direct sequence analysis previously performed on these patients excluded CTG expansion in the *DMPK* gene and *MTM1* mutations. Their clinical history was carefully reviewed. Additional medical information from affected family members was obtained by the attending neurologist, when possible.

2.2. Sequence analysis of DNM2

'All 22 patients and 4 members of 1 family were examined for *DNM2* sequence variants. DNA was extracted from blood or muscle samples using standard protocols. We sequenced all the exons and the exon–intron boundaries of *DNM2*. Both strands of PCR products were sequenced directly using BigDye Terminator v1.1 Sequencing Standard Kit (Applied Biosystems) with an automated ABI 3100 DNA sequencer with custom-made primers (Supplementary Table).

3. Results

3.1. Genetic diagnosis

Among 22 patients, we identified 3 mutations in 4 probands: c.1102G>A (p.E368K), c.1105C>T (p.R369W), and c.1393C>T (p.R465W), all of which were previously reported [6]. We further confirmed the mutations in affected family members of 2 patients (Table 1). We did not identify mutations from the families with consanguinity.

3.2. Clinical features

The clinicopathological features of patients with *DNM2* mutations are shown in Table 1. Clinical information for Patient 1-1 was not available. He was autopsied at the age of 17 years, at which point the gastrocnemius muscle was taken as a sample for analysis (Fig. 1A). The inheritance pattern was compatible with AD transmission in families 2 and 3, while it was sporadic in Patient 4-1.

Patients 2-1 and 3-2 were previously reported to have AD CNM or myotubular myopathy (Fig. 2A) [4,5]. In brief, Patient 2-1 noticed an ankle contracture at the age of 10 years and started having difficulty in climbing stairs at the age of 30 years. Achilles tendon elongation was performed at the age of 37 years, during which this patient was found to have atrophy of facial and distal muscles, and diminished tendon reflexes. He had mild ptosis, but ophthalmoplegia was not observed. Creatine kinase (CK) levels were within the normal range. nEMG was myogenic. Muscle biopsy of the rectus femoris at the age of 42 years showed 68% centrally nucleated fibers and a scattered radial distribution (Fig. 1B). CT of the patient's hamstring, soleus, and gastrocnemius muscles showed atrophy and fatty changes. There was no cardiac or respiratory involvement. Nerve conduction velocities were normal except for low-median compound action potentials that could be explained by muscle atrophy. Patient 2-2 exhibited ankle contracture, *pes cavus* due to plantaris muscle atrophy, and distal atrophy since 10 years of age and also underwent Achilles tendon elongation for ankle contracture in his second decade. No ptosis or ophthalmoplegia was observed.

Patient 3-2 noticed progressive lower-leg weakness, atrophy, and ankle contracture when he was 15 years old and he underwent achillotenotomy at 18 years of age. He developed dyspnea at the age of 54 years that necessitated a tracheotomy at the age of 55 years. Neurological findings at the age of 55 years revealed mild ptosis, distal muscle atrophy and weakness, and mild facial muscle involvement including ptosis. CK level was 48 IU/L. nEMG was myogenic. Sural nerve biopsy was unremarkable. Muscle biopsy of the peroneus brevis showed centrally placed nuclei in 40% of the fibers (Fig. 1C). The patient unfortunately died at the age of 58 years, and the primary cause of death was undetermined. His children (Patients 3-6, 3-7, 3-8, and 3-9 (Fig. 2B)) were found to have *pes cavus* caused by plantar muscle atrophy and were slow runners in their childhood.

At the age of 20 years, Patient 3-6 could not appose his palms when his wrists were extended and at the age of 35 years, he had difficulty in walking. He developed bilateral ankle contracture, because of which he had to stand and walk tiptoed. When he was 50 years old, neurological examination showed distal muscle weakness and atrophy with ankle- and finger-joint contractures (Fig. 3A–D). His deep tendon reflexes were also diminished. He lost his left eye in an accident during his childhood, but neither ophthalmoplegia in his right eye nor ptosis was observed. No peripheral nerve involvement was found on normal nerve conduction study. nEMG was myogenic. Results of echocardiography, Holter ECG, and pulmonary function tests were normal. Muscle biopsy of the biceps brachii at the age of 50 years was compatible with the CNM diagnosis (Fig. 1D–G).

The daughters of Patient 3-6 (Patients 3-10 and 3-11) followed a similar clinical course. They did not have ophthalmoplegia nor ptosis (Fig. 3G). Muscle CT showed marked atrophy in the posterior compartment of the lower extremities (gluteus maximus, hamstrings, gastrocnemius, and soleus) and thigh abductors, while only moderate atrophy and fatty changes were observed in the paraspinal muscles (Fig. 3E). Patient 3-11 had muscle involvement limited to the biceps femoris, gastrocnemius, and soleus as shown on CT at the age of 19 years (Fig. 3F). Both Patients 3-10 and 3-11 showed myogenic changes on nEMG, and the findings of nerve conduction studies were normal.

Patient 4-1 had no obvious family history (Fig. 3C). He noticed ankle contracture at the age of 30 and had gait disturbance at the age of 40 years. He underwent muscle biopsy at the age of 55 years. He was ambulant but did not use a cane. nEMG was actively myogenic, and the results of nerve conduction studies were normal.

In all patients, *pes cavus* caused by plantar muscle atrophy was the earliest sign that appeared before the age of 10 years. Atrophy of calf and posterior thigh muscles was seen during the second decade, but could be detected by muscle CT even in early stages (Fig. 3E and F). The clinical course was relatively benign, except for that of 1 patient who died at the age of 16 years (Patient 1-1), although no detailed information on the cause of death was available. Neither cardiac nor respiratory failure occurred in any patient, except Patient 3-2 who underwent tracheotomy for dyspnea secondary to severe pneumonia. All the 3 patients who were above 50 years of age are still ambulant. With an exception of Patient 3-2,

Table 1
Clinicopathological features of DNM2-CNM.

	Family		1	2			3			4
Demographic data	Patient number		1-1	2-1	3-2	3-6	3-7	3-10	3-11	4-1
	Mutation		c.1102G>A (p.E368K)	c.1393C>T (p.R465W)	c.1105C>T (p.R369W)	c.1105C>T (p.R369W)	c.1105C>T (p.R369W)	c.1105C>T (p.R369W)	c.1105C>T (p.R369W)	c.1105C>T (p.R369W)
	Age/sex		16/M	42/M	55/M	50/M	47/F	22/F	19/F	55/M
Clinical features	Ability to walk		NR	Ambulatory	With cane	With cane	Ambulatory	Ambulatory	Ambulatory	Ambulatory
	Opthalmoplegia		NR	–	–	–	–	–	–	–
	Ptosis		NR	+	+	–	–	–	–	–
	MMT upper extremities	Proximal	NR	5	5	5	4	4	4	4
		Distal	NR	5	5	2	3	2	2	3
	MMT lower extremities	Proximal	NR	4	5	4	3	3	4	4
		Distal	NR	4	5	2	2	2	2	3
	Deep tendon reflexes		NR	–	NR	N	↓	–	NR	↓
	Joint contractures		NR	Elbow, wrist, ankle	Ankle	Finger, wrist, elbow, spine, ankle	Finger, wrist, elbow, spine, ankle	Finger, wrist, elbow, spine, ankle	Finger, wrist, elbow, spine, ankle	Ankle
	Muscle atrophy	Leg	NR	+	+	+	+	+	+	+
		Paraspinal	NR	NR	NR	+	+	+	+	+
		Plantar	NR	+	+	+	+	+	+	+
	Cardiovascular		NR	N	N	NR	NR	N	N	N
	Respiratory		NR	NR	Tracheotomy	Normal vital capacity	Normal vital capacity	Normal vital capacity	Normal vital capacity	NR
	Electromyography		NR	M	M	M	M	M	NT	M
	Nerve conduction studies		NR	*	N	N	N	N	N	NR
	Serum CK		NR	N	N	N	N	NR	N	N
	Muscle CT	Calf	NR	+	+	+	NR	NR	–	+
		Thigh	NR	2+	2+	2+	NR	NR	+	2+
Findings on muscle biopsy	% of centrally nucleated fibers		65	68	55	60				70
	Radial distribution of myofibrils		+	+	NT	+				+
	Type 1 predominance (%)		80	79	NT	88				90
	Type 1 atrophy		+	+	NT	+				+
	Type 2B deficiency		+	+	NT	+				+
	Type 2C fibers (%)		2	1	NT	2				5

Abbreviations: MMT, manual muscle testing; +, present; –, absent; N, normal; NR, no record; NT, not tested; ↓, decreased; EMG, electromyography; M, myogenic changes; and NCS, nerve conduction study. The CT scores are as follows: 1+: decreased signal density and 2+: decreased signal density with severe muscle atrophy.

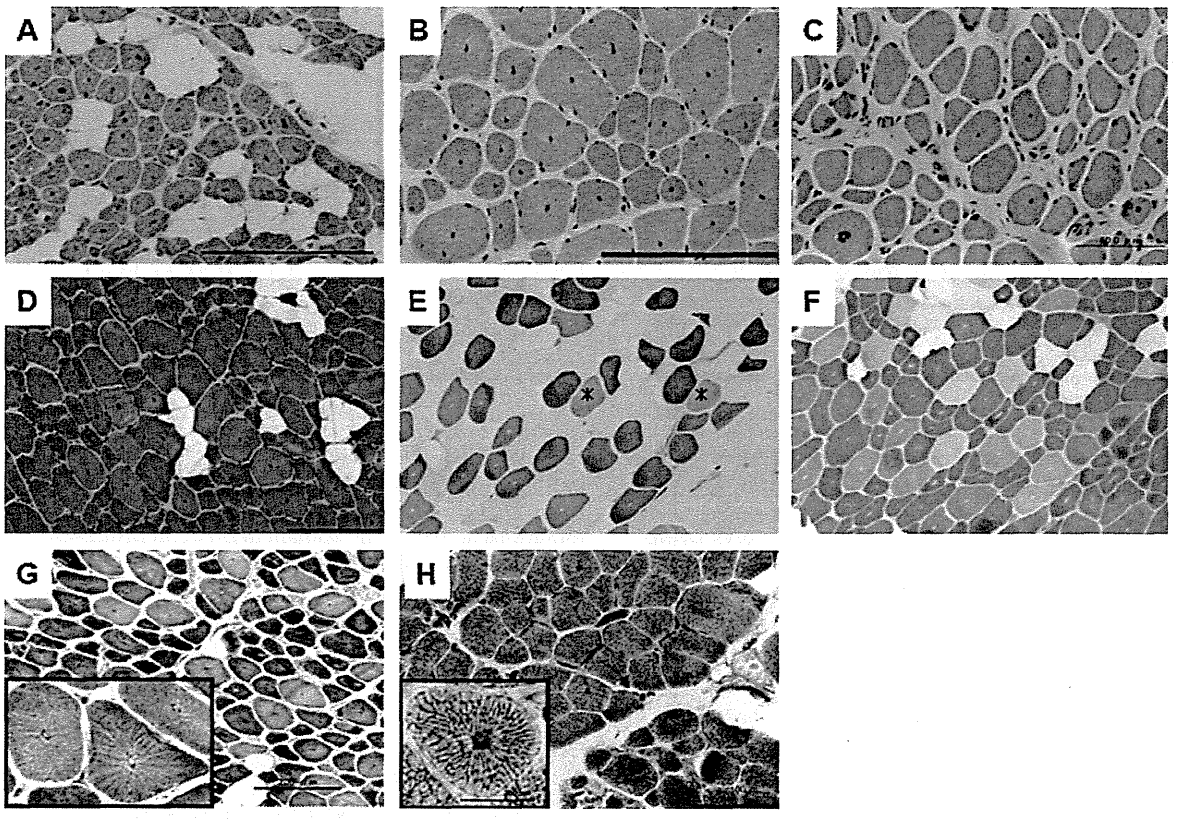

Fig. 1. Biopsy findings of DNM2-CNM (A-G) and non-DNM2-CNM (H). Hematoxylin and eosin stain of muscle sections from Patients 1-1 (A), 2-1 (B), 3-2 (C), and 3-6 (D). Numerous centronuclear fibers (up to 55%) and interstitial fibrosis were observed. Histochemical findings in muscle sections from Patient 3-6 (E–G). Type 1 predominance and hypotrophy (E, ATPase staining pH 10.6), a few type 2C fibers (F, ATPase pH 4.6), and radial distributions (G, NADH-TR) were observed. Radial distributions were also observed in some non-DNM2-CNM muscles (H, NADH-RT).

neither ptosis nor ophthalmoplegia was observed in the affected family members.

Clinical features of the CNM patients without *DNM2* mutations (non-DNM2-CNM) along with the number of patients are given below: proximal weakness (2/18), floppy infant (8/18), scoliosis (1/18), mental retardation (1/18), dysphagia (1/18), myalgia (1/18), and high-arched palate (8/10). Furthermore, only 1 of 10 patients with non-DNM2-CNM showed joint contracture. The clinical features of non-DNM2-CNM varied more widely than those of DNM2-CNM.

3.3. Summary of the pathological features

In all patients with DNM2-CNM, the pathological findings were rather similar: (1) radial distribution of myofibrils in scattered fibers, (2) type 1 fiber atrophy, (3) type 1 fiber predominance, and (4) a small number of type 2C fibers (Table 1, Fig. 1). In addition, the frequency with which muscle fibers with centrally placed nuclei were observed in DNM2-CNM patients was 63.1 ± 6.1% (mean ± SD), range, 55–70%, which is much lower than that observed in non-DNM2-CNM patients (24.7 ± 13.2%, range, 8–50%).

In contrast, none of the non-DNM2-CNM patients had all the 4 abovementioned pathological features. Definite radial distribution of myofibrils was seen only in 2 of 18 cases. In 4 of 18 cases, equivocal radial distribution was observed. Among the 18 cases, type 1 fiber atrophy was noted in 12 patients; type 1 fiber predominance, in 16 patients; and type 2C fibers, in 12 patients. In addition, type 2 fiber atrophy was seen in 2 of 18 patients.

4. Discussion

This is the first report to document *DNM2* mutations in CNM patients in Japan with a low frequency, similar to the cases found in Europe, the United States, Central Africa, and Argentina [7,10,11]. All affected family members had distal muscle atrophy, finger and ankle contractures, and *pes cavus* caused by plantar muscle atrophy in their childhood (Table 1, Fig. 3A–D). Atrophy and fatty changes in the gastrocnemius muscle were the earliest signs observed on CT and were noted in the second decade of their lives (Fig. 3E). Thigh flexor, gluteus maximus, and paraspinal muscles were involved in the later stages (Fig. 3F).

The clinical and pathological features of DNM2-CNM were rather homogeneous in our series, as in previous reports [6,10,16]. This can be helpful in establishing a working diagnosis in CNM patients. The phenotypes of the mutations identified here (E368K, R465W) were almost identical to those identified in previous cases [7], although only 1 patient with E368K and 1 with R369W showed ptosis and ophthalmoplegia. In addition, the early death of Patient 1-1 and the respiratory failure of Patient 3-2 are unusual occurrences for DNM2-CNM, although we could not obtain detailed information.

A high occurrence of ptosis (9/10 [10], 7/11 [18]) and ophthalmoplegia (2/10 [10], 5/11 [18]) among DNM2-CNM patients is observed in other countries [10], while in our series, ptosis was much more rare (2/8), and ophthalmoplegia was not seen in our

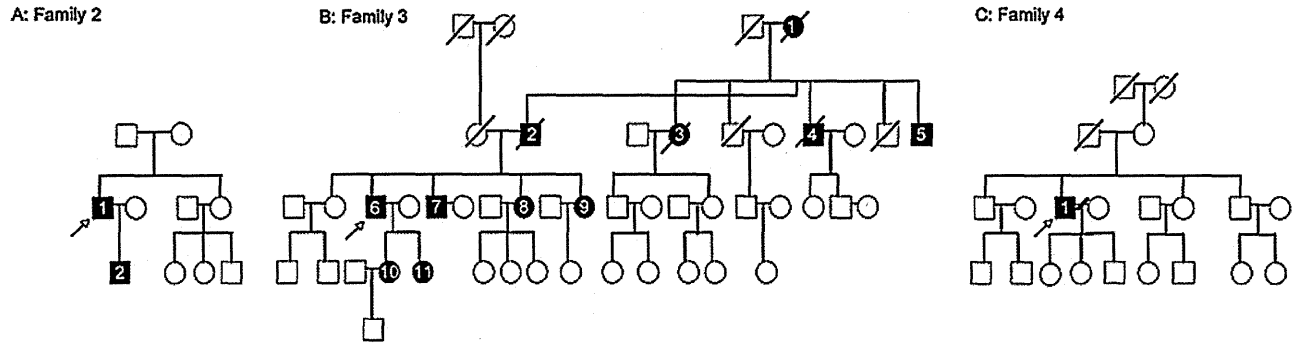

Fig. 2. The DNM2-CNM family tree. Families 2 and 3 had obvious autosomal dominant inheritance. On the contrary, Patient 4-1 had a sporadic onset. His parents and children did not show any symptoms.

cohort. In previous studies, most patients who did not have ptosis and ophthalmoplegia were from a p.R522H family, and most of them were infants [17]. The Japanese patients in our study, including those with the p.R465W mutation that causes DNM2-CNM with ptosis and ophthalmoplegia, as shown in a European study, did not have ophthalmoplegia, and only 2 (p.R465W and R369W) patients exhibited ptosis. Ethnic background may be a contributing factor to the occurrence of ptosis because there are some anatomical differences between the eyelids of Asian and European populations: Asians have shallower eyelids than Europeans [18,19]. Since the severity of ptosis is correlated to the severity of myopathy, ptosis caused by mutations in the middle domain in *DNM2* in DNM2-CNM patients could be mild enough not to be recognized in the eyelids of Asians.

On the other hand, among non-DNM2-CNM patients, ptosis or ophthalmoplegia was also seen in 4 of 18 cases, suggesting that ocular symptoms may not be a specific indicator of *DNM2* mutations

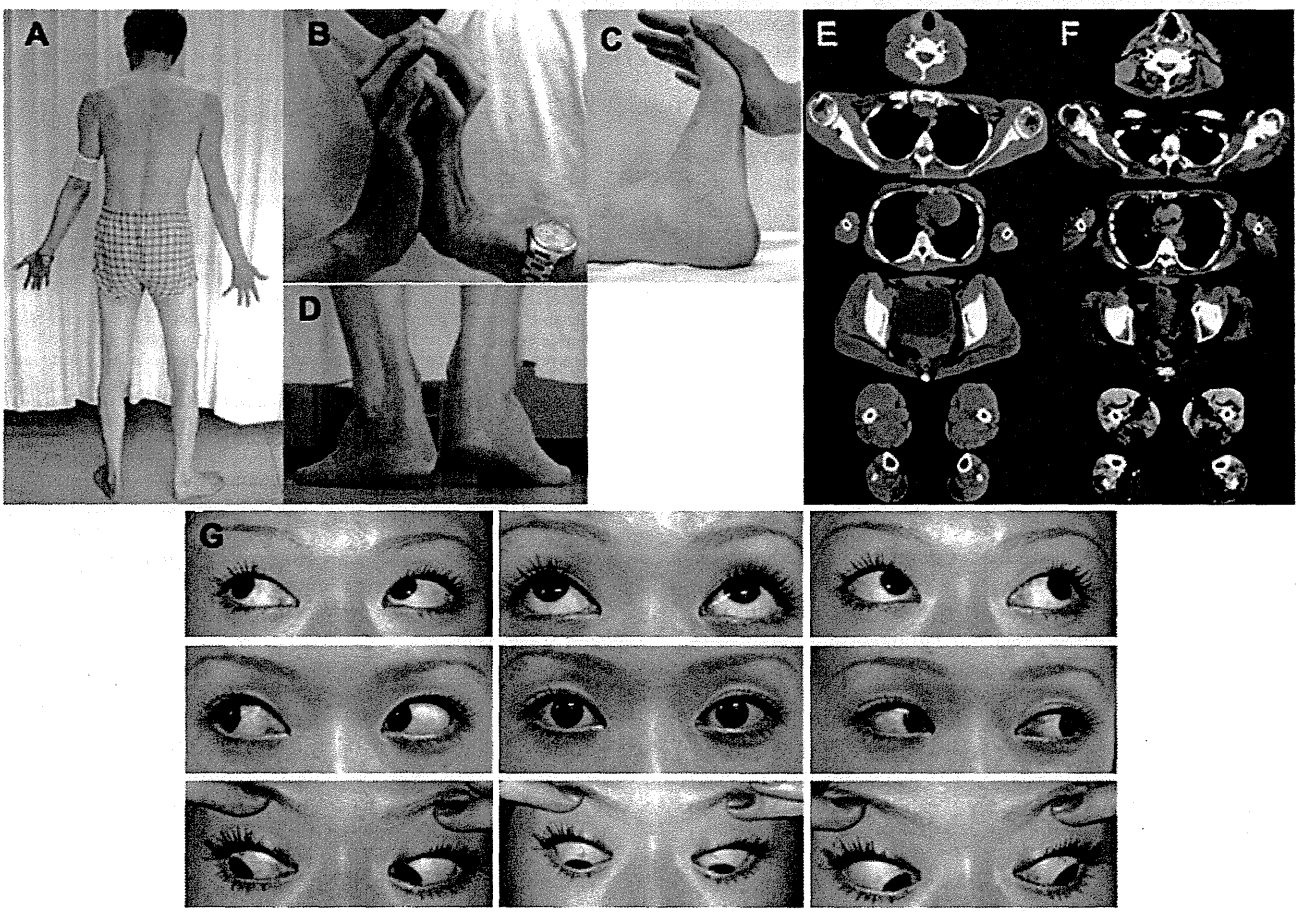

Fig. 3. Photograph of Patient 3-6: distal muscular atrophy (A), joint contracture of fingers (B), and ankle contracture (C); patient could not put his heels on the floor because of the ankle contracture (D). Muscle CT of Patient 3-6 (F) and Patient 3-11 (E) depicting lower-leg muscle atrophy of the posterior compartment (gluteus maximus, hamstrings, gastrocnemius, and soleus), thigh abductor, and paraspinal muscles. Note the early involvement of the biceps femoris, gastrocnemius, and soleus in Patient 3-11 when she was 19 years old. Ophthalmoplegia and ptosis are not observed in most patients (G: Patient 3-11).

in CNM patients, at least in Japanese patients, further highlighting the importance of the frequency of ocular involvement as a genetic factor.

Other symptoms of the central nervous system and peripheral neuropathy were also observed in our cohort and were reported as subtle complications of DNM2-CNM [17]. Among the non-DNM2-CNM patients, other causative genes for CNM were considered. *MTM1* mutations are implicated in CNM, but in our cohort, *MTM1* mutations were excluded. Compound heterozygous mutations in *hJUMPY*, a gene that encodes a phosphoinositide phosphatase, were reported as a cause of sporadic CNM [8]. Additionally, *BIN1* is a newly identified causative gene for autosomal recessive CNM [9]; patients with autosomal recessive CNM show typical CNM muscle pathology and proximal-dominant muscle weakness, which is more severe than observed in DNM2-CNM patients. The pathology of CNM with *BIN1* mutations does not have a radial distribution, which is thought to be a hallmark of DNM2-CNM [9]. Notably, some of our non-DNM2-CNM patients showed a radial distribution. However, none of our non-DNM2-CNM patients had a family history that would indicate autosomal recessive inheritance and merit further mutational analysis of the *hJUMPY* and *BIN1* genes. Other candidate genes include *Srpk3* [20] and *PTPLA* [21], which were thus far implicated as causative genes of CNM in mice and dogs.

DNM2 mutations were also identified in AD Charcot–Marie–Tooth disease (CMT) [22]; in fact, some DNM2-CNM patients also show very mild reductions in nerve conduction velocities in the lower legs [10] or pathological changes in both myelinated and unmyelinated nerve fibers [18]. Nevertheless, none of our patients showed any abnormality in nerve conduction studies, suggesting that peripheral nerve involvement does not occur frequently in DNM2-CNM patients.

Although the precise pathomechanism of DNM2-CNM is not known, mutations are thought to hinder either the transport of DNM2 to the centrosome or its interaction with some centrosomal component [7]. Interestingly, in our study and past reports of *DNM2* mutations in the middle domain, characteristic features were observed in muscle pathology, as opposed to neonatal DNM2-CNM with PH domain mutations in which centrally nucleated fibers and radial distribution of myofibers are less prominent [11].

Acknowledgements

This work was supported in part by Research on Intractable Diseases of Health and Labour Sciences Research Grants, Comprehensive Research on Disability Health and Welfare, Health and Labour Science Research Grants, Intramural Research Grant (23-5 23-4) for Neurological and Psychiatric Disorders of NCNP and Young Investigator Fellowship from Translational Medical Center, National Center of Neurology and Psychiatry.

Appendix A. Supplementary data

Supplementary data associated with this article can be found, in the online version, at doi:10.1016/j.clineuro.2011.10.040.

References

[1] North K. In: Engel AG, Franzini-Armstrong C, Myology, editors. Congenital myopathies. 3rd ed. New York: McGraw-Hill; 2004. p. 1494–5.
[2] Jeannet PY, Mittaz L, Dunand M, Laforêt P, Urtizberea JA, Rouche A, et al. Clinical and histologic findings in autosomal centronuclear myopathy. Neurology 2004;11:1484–90.
[3] Wallgren-Petterson C, Clarke A, Samson F, Fardeau M, Dubowitz V, Moser H, et al. The myotubular myopathies: differential diagnosis of the X linked recessive, autosomal dominant, and autosomal recessive forms and present state of DNA studies. J Med Genet 1995;32:673–9.
[4] Sakuma T, Nakajima H, Fujimura C, Kimura F, Hanabusa T. A case of centronuclear myopathy with Charcot–Marie–Tooth disease-like lower leg muscle atrophy. Naika 2004;54:192–4 [in Japanese].
[5] Wakabayashi Y, Arimura Y, Sawaguchi Y, Koike F, Yoshino K. A case of myotubular myopathy with autosomal dominant inheritance. No to Shinkei 1980;32:715–22 [in Japanese].
[6] Bitoun M, Bevilacqua JA, Eymard B, Prudhon B, Fardeau M, Guicheney P, et al. A new centronuclear myopathy phenotype due to a novel dynamin 2 mutation. Neurology 2009;6:93–5.
[7] Bitoun M, Maugenre S, Jeannet PY, Lacène E, Ferrer X, Laforêt P, et al. Mutations in dynamin 2 cause dominant centronuclear myopathy. Nat Genet 2005;37:1207–9.
[8] Tosch V, Rohde HM, Tronchère H, Zanoteli E, Monroy N, Kretz C, et al. A novel PtdIns3P and PtdIns (3,5) P_2 phosphatase with an inactivating variant in centronuclear myopathy. Hum Mol Genet 2006;1:3098–106.
[9] Nicot AS, Toussaint A, Tosch V, Zanoteli E, Monroy N, Kretz C, et al. Mutations in *amphiphysin 2* (*BIN1*) disrupt interaction with dynamin 2 and cause autosomal recessive centronuclear myopathy. Nat Genet 2007;39:1134–9.
[10] Fischer D, Herasse M, Bitoun M, Barragán-Campos HM, Chiras J, Laforêt P, et al. Characterization of the muscle involvement in dynamin 2-related centronuclear myopathy. Brain 2006;129:1463–9.
[11] Bitoun M, Bevilacqua JA, Prudhon B, Barragán-Campos HM, Chiras J, Laforêt P, et al. Dynamin 2 mutations cause sporadic centronuclear myopathy with neonatal onset. Ann Neurol 2007;6:666–70.
[12] Jones SM, Howell KE, Henley JR, Cao H, McNiven MA. Role of dynamin in the formation of transport vesicles from the trans-Golgi network. Science 1998;23:573–7.
[13] Schafer DA, Weed SA, Binns D, Karginov AV, Parsons JT, Cooper JA. Dynamin2 and cortactin regulate actin assembly and filament organization. Curr Biol 2002;29:1852–7.
[14] Thompson HM, Cao H, Chen J, Euteneuer U, McNiven MA. Dynamin 2 binds gamma-tubulin and participates in centrosome cohesion. Nat Cell Biol 2004;6:335–42.
[15] Schessl J, Medne L, Hu Y, Zou Y, Brown MJ, Huse JT, et al. MRI in *DNM2*-related centronuclear myopathy: evidence for highly selective muscle involvement. Neuromuscul Disord 2007;17:28–32.
[16] Jeub M, Bitoun M, Guicheney P, Kappes-Horn K, Strach K, Druschky KF, et al. Dynamin 2-related centronuclear myopathy: clinical, histological and genetic aspects of further patients and review of the literature. Clin Neuropathol 2008;27:430–8.
[17] Echaniz-Laguna A, Nicot AS, Carré S, Franques J, Tranchant C, Dondaine N, et al. Subtle central and peripheral nervous system abnormalities in a family with centronuclear myopathy and a novel dynamin 2 gene mutation. Neuromuscul Disord 2007;17:955–9.
[18] Susman RD, Quijano-Roy S, Yang N, Webster R, Clarke NF, Dowling J, et al. Expanding the clinical, pathological and MRI phenotype of *DNM2*-related centronuclear myopathy. Neuromuscul Disord 2010;20:229–37.
[19] Liu D, Hsu WM. Oriental eyelids. Anatomic difference and surgical consideration. Ophthal Plast Reconstr Surg 1986;2:59–64.
[20] Nakagawa O, Arnold M, Nakagawa M, Hamada H, Shelton JM, Kusano H, et al. Centronuclear myopathy in mice lacking a novel muscle-specific protein kinase transcriptionally regulated by MEF2. Genes Dev 2005;19:2066–77.
[21] Pele M, Tiret L, Kessler JL, Blot S, Panthier JJ. SINE exonic insertion in the PTPLA gene leads to multiple splicing defects and segregates with the autosomal recessive centronuclear myopathy in dogs. Hum Mol Genet 2005;1:1417–27.
[22] Züchner S, Noureddine M, Kennerson M, Verhoeven K, Claeys K, De Jonghe P, et al. Mutations in the pleckstrin homology domain of dynamin 2 cause dominant intermediate Charcot-Marie-Tooth disease. Nat Genet 2005;37:289–94.

Available online at www.sciencedirect.com

SciVerse ScienceDirect

American Journal of OTOLARYNGOLOGY

ELSEVIER

American Journal of Otolaryngology–Head and Neck Medicine and Surgery 33 (2012) 758–761

www.elsevier.com/locate/amjoto

Case reports

Videofluorographic detection of anti–muscle-specific kinase–positive myasthenia gravis

Toshiyuki Yamamoto, MD, PhD*, Norio Chihara, MD, Madoka Mori-Yoshimura, MD, PhD, Miho Murata, MD, PhD

Department of Neurology, National Center Hospital of Neurology and Psychiatry, Tokyo, Japan

Received 19 March 2012

Abstract A 47-year-old woman with dysphagia and ptosis gradually developed dysarthria and muscular weakness. Magnetic resonance imaging, testing for anti–acetylcholine receptor antibodies, edrophonium chloride (EC) test, and electrophysiologic test revealed no abnormalities. A psychogenic reaction was suspected. Four months after disease onset, the patient presented to our hospital. In videofluoroscopic examination of swallowing (VF), there was no aspiration for swallowing of either liquid or soft food. It revealed, however, poor pharyngeal constriction, no epiglottis inversion, repeated swallowing movements, and large amounts of pharyngeal residue. Videofluoroscopic examination of swallowing after an intravenous injection of 10 mg EC showed improvements in all above observations; particularly, it was clear when swallowing soft food. Furthermore, the anti–muscle-specific kinase (MuSK) antibody titer was elevated, and anti-MuSK antibody–positive myasthenia gravis (MuSK-MG) was diagnosed. Thus VF during EC test may be helpful in diagnosing MuSK-MG in patients with dysphagia.

1. Introduction

Myasthenia gravis (MG) that is positive for anti–muscle-specific kinase (MuSK) (MuSK-MG) accounts for only 27% to 38% of anti–acetylcholine receptor (AChR) antibody–negative MG. Muscle-specific kinase MG is associated with bulbar symptoms, such as dysphagia and dysarthria, from an early stage [1-3]; therefore, these patients often present with the chief complaint of difficulty in swallowing. They need to consult an otolaryngologist before a definite diagnosis of MuSK-MG is made because MuSK antibody titer is measured in only some laboratories. The edrophonium chloride (EC) test, which evaluates the improvement of muscle weakness after intravenous EC injection, is positive in only 65.6% of patients with MuSK-MG in contrast to 88.6% of patients with anti–AChR antibody–positive MG (AChR-MG) [1,4].

Videofluoroscopic examination of swallowing (VF) before and after intravenous EC injection is useful for the evaluation of dysphagia during the course of AChR-MG [5,6]; however, whether it contributes to the diagnosis of MuSK-MG is unknown. This is the first case report that describes changes in swallowing movements before and after EC injection in a patient with MusK-MG.

2. Case report

A 47-year-old woman with dysphagia, dysarthria, ptosis, and general muscular weakness gradually developed difficulty in speaking and bilateral ptosis 1 month after the onset of difficulty in swallowing. Her medical, lifestyle, and family history were unremarkable.

The findings for cranial magnetic resonance imaging (MRI), neck MRI, and laboratory investigations were normal. The EC test was negative, and the cause of her symptoms

* Corresponding author. Department of Neurology, National Center Hospital of Neurology and Psychiatry, 4-1-1 Ogawahigashi-cho, Kodaira City, Tokyo 187-8551, Japan. Tel.: +81 42 341 2711; fax: +81 42 346 1705.
E-mail address: yamamoto@ncnp.go.jp (T. Yamamoto).

0196-0709/$ – see front matter © 2012 Elsevier Inc. All rights reserved.
http://dx.doi.org/10.1016/j.amjoto.2012.04.003

remained undiagnosed. At 2 months after symptom onset, the patient experienced choking while drinking water, could raise both arms only to the shoulder level, and had to hold on to railings when climbing stairs. After 3 months, she developed drooping of the neck (muscle weakness). The repetitive nerve stimulation test gave normal results, and the anti-AChR antibody test was negative; therefore, a psychogenic reaction was suspected. After 4 months, she presented to our hospital for the evaluation of dysphagia.

Blood pressure was 108/76 mm Hg, and the pulse was 86 per minute and regular. There was no respiratory distress, and the SpO_2 was 99%. Consciousness was intact. The patient complained of difficulty in chewing and swallowing food. Bilateral ptosis was observed. Hypernasality was noted with poor bilateral soft palate elevation. Facial muscle strength was decreased, and cheek puffing could not be maintained. Tongue protrusion was in the midline, and there was no atrophy or muscular fasciculation of the tongue. The gag reflex was intact. The proximal muscle groups were weaker than the distal muscle groups, with no left-right difference. No diurnal variations in muscle strength were observed. Tendon reflexes were decreased, and no pathologic reflexes were noted. Autonomic nervous symptoms, sensory disturbances, and cerebellar ataxia were not noted. Laboratory investigations, including thyroid function and creatine kinase levels, were normal. Respiratory functions and electrocardiogram were also normal.

We performed all x-ray fluoroscopic examinations after obtaining the patient's written informed consent, and the x-ray fluoroscopy time was less than 5 minutes. We evaluated the swallowing motion using 10 mL of 2-fold diluted 110% wt/vol barium solution (liquid) and 8 g of barium corned beef (soft food). The same evaluation was repeated after intravenous injection of 10 mg EC. All swallowing motions were recorded on DVD at 30 frames per second, and after the test, 1 examiner analyzed all VF clips using PC software Move-tr/2D 7.0 (Library Inc., Tokyo, Japan) and Adobe Photoshop CS5 (Adobe Systems Ins., San Jose, CA, USA).

The pharyngeal area before the start of swallowing (PA hold) [7] was 13.4 cm^2. On VF before EC injection, the liquid in the oral cavity could not be retained by the tongue and soft palate. Pharyngeal constriction during swallowing was poor, and the maximum pharyngeal constriction (PA max) [7] was 5.1 cm^2 with a pharyngeal constriction ratio (PCR) [7] of 0.38 (normal, 0.03 ± 0.03) [8]. The soft palate did not elevate, and the epiglottis did not invert (Fig, A). Liquid reflux into the mouth was noted. There was no aspiration for either liquid or soft food swallowing. After swallowing, both the liquid and the soft food remained in the epiglottic vallecula and piriform sinus. In particular, soft food residues remained at the base of the tongue and posterior hypopharyngeal wall (Fig, B). The pharyngeal transit duration (PTD) [9] for the soft food was 8.06 seconds. The number of swallows for the liquid was 8, whereas that for the soft food was 10.

On VF after EC injection, oral retention of the liquid was possible, and pharyngeal constriction improved. The PA max was 3.2 cm^2, and the PCR was 0.23. The soft palate did not elevate, but the epiglottis did invert (Fig, C). The PTD of the soft food improved to 6.15 seconds. There was no aspiration of the liquid or the soft food. The number of swallows decreased to 4 for the liquid and soft food each, and pharyngeal residues also decreased (Fig, D; Table). The patient was aware of the improvement in swallowing function after EC injection while consuming the soft food.

The anti-MuSK antibody titer was 10.03 nmol/L (normal, ≤ 0.05 nmol/L), and this led to a definitive diagnosis. The patient underwent 6 sessions of plasma adsorption therapy, and therapy with prednisolone 30 mg/d and tacrolimus 3.0 mg/d was initiated. The VF during treatment demonstrated that pharyngeal constriction was improved. When swallowing liquid, the number of swallows was 2; PA hold, 12.2 cm^2; PA max, 1.8 cm^2; and PCR, 0.15. When swallowing soft food, the number of swallows was 3; and PTD, 1.03 seconds. The pharyngeal residues of the liquid and the soft food decreased, but soft palate elevation remained moderately weak. The patient was aware of an improvement in swallowing function and was gradually able to eat normal diet. Muscle weakness and bilateral ptosis also improved, but mild hypernasality remained.

3. Discussion

In general, in swallowing liquids, there is a strong component of passive transport resulting from gravity, whereas active transport by tongue muscle retropulsion and pharyngeal muscle constriction has a greater role in swallowing soft foods [10]. In this patient, comparisons of the PA max and PCR before and after EC injection provided meaningful results in quantitative analysis. These improvements were due to temporary improvements in muscular strength with EC injection. For the soft food, the changes in PTD and improvement in pharyngeal retention were more obvious than for the liquid, suggesting abnormal active transport. Because of longer PTD, the change in swallowing soft food was more easily recognizable. The patient's awareness of the improvement in swallowing function after EC injection was also more apparent for soft food as with liquids. Our findings thus suggest that VF examination for soft food after intravenous EC injection would aid in diagnosing MuSK-MG even in the absence of abnormalities on electrophysiologic and laboratory tests.

In 70% of MuSK-MG patients, low doses of anticholinesterase drugs are effective; however, in 8.8% of MuSK-MG patients, a cholinergic crisis occurs despite these medications [11]. When performing VF after EC injection in MuSK-MG patients taking an anticholinesterase drug, the swallowing function may transiently worsen. Videofluoroscopic examination of swallowing during the EC test may be useful for differentiating MuSK-MG from other diseases that cause a bulbar syndrome; however, further studies are needed for evaluating the safety of this procedure.

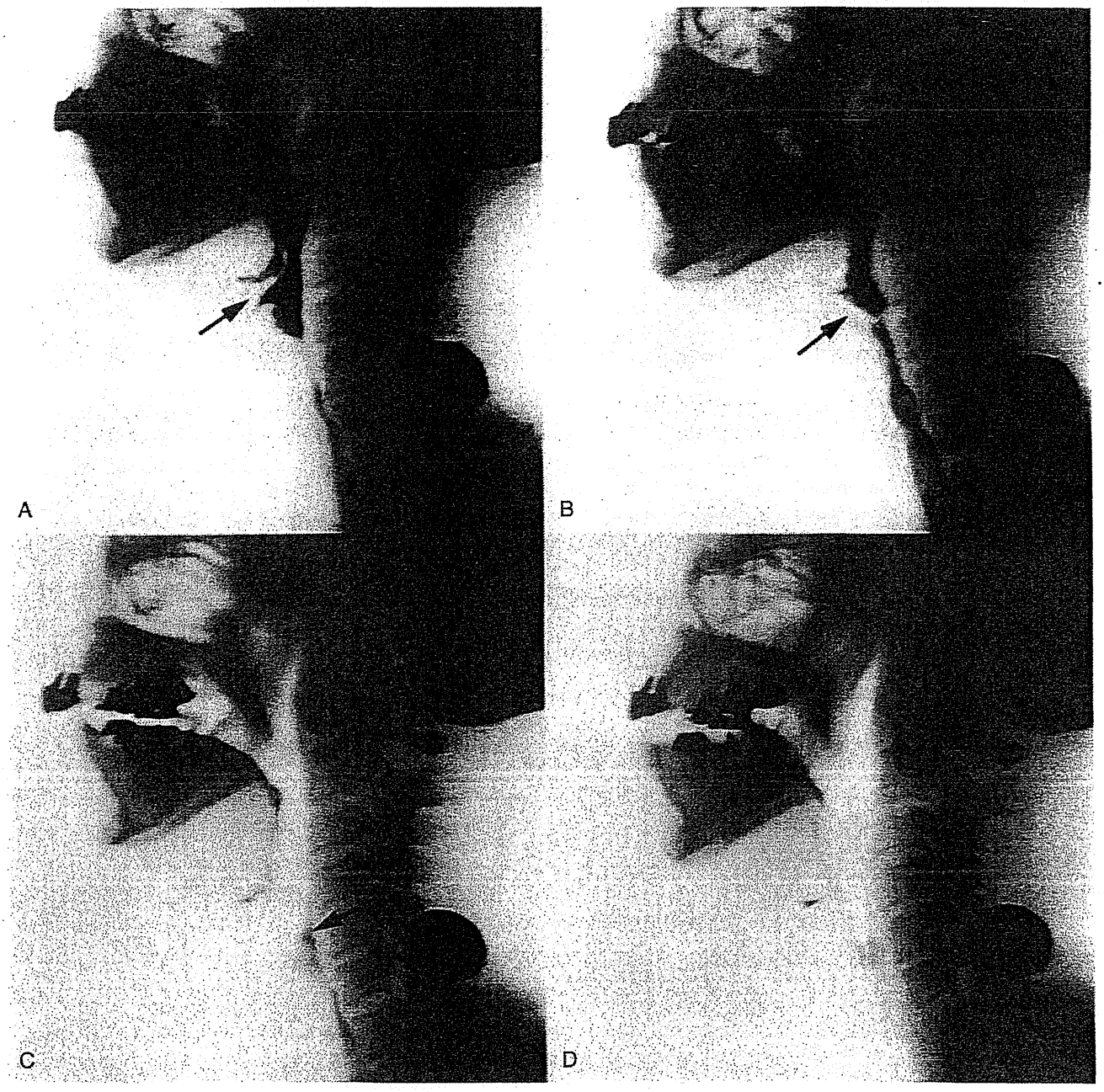

Fig. Videofluorography before and after intravenous injection of EC. A and C, Before EC injection. B and D, After EC injection. A and B, Maximum pharyngeal constriction during swallowing the liquid. C and D, Pharyngeal residue after swallowing the soft food. During swallowing the liquid before EC injection, the epiglottis did not invert at the point of maximum pharyngeal constriction (A, arrow), and pharyngeal constriction was insufficient, resulting in poor passage. After EC injection, although pharyngeal constriction was insufficient, the epiglottis inverted (B, arrow). When swallowing the soft food before intravenous EC, residue remained at the base of the tongue, epiglottic vallecula, piriform fossa, and posterior hypopharyngeal wall (C, arrow), whereas after EC injection, the pharyngeal residue was lesser (D). The circle in the figure is a marker for the maximum diameter of 23.5 mm.

This patient was originally suspected of having a psychogenic reaction before the swallowing function was evaluated. The diagnosis of psychogenic dysphagia should be made with caution and only after comprehensive evaluations [12]. Atrophy of the tongue muscles in early-stage MuSK-MG is often observed on MRI [13,14]. In this patient, atrophy from the tongue base to the pharynx was observed in the lateral view during x-ray fluoroscopy; this would be one of the useful findings to distinguish organic dysphagia from a psychogenic reaction, and it can be evaluated in a consulting room using an indirect laryngoscope. When patients with a chief complaint of dysphagia

Table
Comparison of videofluorography findings before and after EC injection

	Measurement parameter	Before EC injection	After EC injection
With liquid	PCR	0.38	0.23
	No. of swallows	8	4
	Soft palate elevation	None	None
	Epiglottis inversion	None	Present
	Pharyngeal residues	–	–
With soft food	No. of swallows	10	4
	PTD (s)	8.06	6.15
	Pharyngeal residues	–	–

have abnormal findings that suggest glossopharyngeal muscle weakness or atrophy, evaluation of swallowing after EC injection is advisable even if aspiration is not found in VF. This process might lead to a timely diagnosis of MuSK-MG, enabling the physician to take appropriate and timely therapeutic decisions.

4. Conflicts of interest

The authors declare that they have no conflicts of interest.

5. Ethics committee approval

All tests in this report were carried out in the normal course of medical treatment. Therefore, we did not apply for ethics committee approval.

6. Patient consent

Written informed consent regarding the submission of this article was obtained from the patient.

Acknowledgments

The authors thank Masakatsu Motomura of the First Department of Clinical Neuroscience and Neurology, Graduate School of Biomedical Sciences, Nagasaki University, Japan for measurement of the anti-MuSK antibody titers.

References

[1] Ohta K, Shigemoto K, Fujinami A, et al. Clinical and experimental features of MuSK antibody positive MG in Japan. Eur J Neurol 2007; 14:1029-34.
[2] Evoli A, Tonali PA, Padua L, et al. Clinical correlates with anti-MuSK antibodies in generalized seronegative myasthenia gravis. Brain 2003; 126:2304-11.
[3] Pasnoor M, Wolfe GI, Nations S, et al. Clinical findings in MuSK-antibody positive myasthenia gravis: a U.S. experience. Muscle Nerve 2010;41:370-4.
[4] Wolfe GI, Oh SJ. Clinical phenotype of muscle-specific tyrosine kinase-antibody–positive myasthenia gravis. Ann N Y Acad Sci 2008; 1132:71-5.
[5] Higo R, Nito T, Tayama N. Videofluoroscopic assessment of swallowing function in patients with myasthenia gravis. J Neurol Sci 2005;231:45-8.
[6] Schwartz DC, Waclawik AJ, Ringwala SN, et al. Clinical utility of videofluorography with concomitant Tensilon administration in the diagnosis of bulbar myasthenia gravis. Dig Dis Sci 2005;50:858-61.
[7] Leonard R, McKenzie S. Dynamic swallow study: instrumentation and measurement techniques. In: Leonard R, & Kendall K, editors. Dysphagia assessment and treatment planning: a team approach. San Diego, CA: Singular Publishing Group Inc.; 2008. p. 285-8.
[8] Leonard R, Rees CJ, Belafsky P, et al. Fluoroscopic surrogate for pharyngeal strength: the pharyngeal constriction ratio (PCR). Dysphagia 2009;26:13-7.
[9] Robbins JA, Logemann JA, Kirshner HS. Swallowing and speech production in Parkinson's disease. Ann Neurol 1986;19:283-7.
[10] Palmer JB. Bolus aggregation in the oropharynx does not depend on gravity. Arch Phys Med Rehabil 1998;79:691-6.
[11] Evoli A, Bianchi MR, Riso R, et al. Response to therapy in myasthenia gravis with anti-MuSK antibodies. Ann N Y Acad Sci 2008;1132: 76-83.
[12] Ravich WJ, Wilson RS, Jones B, et al. Psychogenic dysphagia and globus: reevaluation of 23 patients. Dysphagia 1989;4:35-8.
[13] Zouvelou V, Rentzos M, Toulas P, et al. MRI evidence of early muscle atrophy in MuSK positive myasthenia gravis. J Neuroimaging 2011; 21:303-5.
[14] Farrugia ME, Robson MD, Clover L, et al. MRI and clinical studies of facial and bulbar muscle involvement in MuSK antibody-associated myasthenia gravis. Brain 2006;129:1481-92.

$CCR2^+CCR5^+$ T Cells Produce Matrix Metalloproteinase-9 and Osteopontin in the Pathogenesis of Multiple Sclerosis

Wakiro Sato,*,[1] Atsuko Tomita,*,†,[1,2] Daijyu Ichikawa,* Youwei Lin,*,‡,§ Hitaru Kishida,† Sachiko Miyake,*,§ Masafumi Ogawa,‡,§ Tomoko Okamoto,‡,§ Miho Murata,‡ Yoshiyuki Kuroiwa,† Toshimasa Aranami,*,§ and Takashi Yamamura*,§

Multiple sclerosis (MS) is a demyelinating disease of the CNS that is presumably mediated by $CD4^+$ autoimmune T cells. Although both Th1 and Th17 cells have the potential to cause inflammatory CNS pathology in rodents, the identity of pathogenic T cells remains unclear in human MS. Given that each Th cell subset preferentially expresses specific chemokine receptors, we were interested to know whether T cells defined by a particular chemokine receptor profile play an active role in the pathogenesis of MS. In this article, we report that $CCR2^+CCR5^+$ T cells constitute a unique population selectively enriched in the cerebrospinal fluid of MS patients during relapse but not in patients with other neurologic diseases. After polyclonal stimulation, the $CCR2^+CCR5^+$ T cells exhibited a distinct ability to produce matrix metalloproteinase-9 and osteopontin, which are involved in the CNS pathology of MS. Furthermore, after TCR stimulation, the $CCR2^+CCR5^+$ T cells showed a higher invasive potential across an in vitro blood–brain barrier model compared with other T cells. Of note, the $CCR2^+CCR5^+$ T cells from MS patients in relapse are reactive to myelin basic protein, as assessed by production of IFN-γ. We also demonstrated that the $CCR6^-$, but not the $CCR6^+$, population within $CCR2^+CCR5^+$ T cells was highly enriched in the cerebrospinal fluid during MS relapse ($p < 0.0005$) and expressed higher levels of IFN-γ and matrix metalloproteinase-9. Taken together, we propose that autoimmune $CCR2^+CCR5^+$ $CCR6^-$ Th1 cells play a crucial role in the pathogenesis of MS. *The Journal of Immunology*, **2012, 189: 5057–5065.**

Multiple sclerosis (MS) is an inflammatory demyelinating disease of the CNS that is presumably mediated by $CD4^+$ T cells reactive to myelin Ag, such as myelin basic protein (MBP) (1). Approximately two thirds of patients with MS have relapsing-remitting MS (RR-MS), which is characterized by acute episodes of exacerbations followed by partial or complete recovery. Although there are periods of remission in the RR-MS stage, a proportion of patients enters a stage of secondary progressive MS decades after the onset of MS. There are no real periods of remission in secondary progressive MS, in which neurodegeneration can be the major cause of irreversible neurologic disability (2).

It is proposed that an initiation of relapse in RR-MS is preceded by activation of autoimmune $CD4^+$ T cells in the peripheral lymphoid organs. These T cells that are potentially reactive to myelin Ag could be activated in response to cross-reactive Ag that are generated by microbial infections (3) or following exposure to proinflammatory factors, such as osteopontin (OPN) (4), thereby acquiring the ability to migrate and infiltrate into the CNS (5, 6). The study performed in experimental autoimmune encephalomyelitis (EAE) showed that activated MBP-specific T cells first reach subarachnoid spaces filled with the cerebrospinal fluid (CSF) after crossing the endothelial barrier. After encountering perivascular APC presenting myelin Ag, the autoimmune T cells are reactivated and produce proinflammatory cytokines, such as IFN-γ and IL-17, as well as proteases, including matrix metalloproteinase (MMP)-9 (7). The proteases degrade components of the basement membranes, leading to the disruption of the blood–brain barrier (BBB). The T cells may invade into the parenchyma through the disrupted area of the BBB and cause CNS inflammation (8).

Research on EAE demonstrated that both IFN-γ–producing Th1 and IL-17–producing Th17 cells could cause inflammatory pathology in the CNS (9, 10). Although characterization of pathogenic T cells in EAE has ignited a search for similar cells in humans, the identity of pathogenic T cells in MS has not been established (10). Recent studies showed the involvement of Th17 cells (11) and of T cells producing both IFN-γ and IL-17 in the pathology of MS (12). However, because the administration of

*Department of Immunology, National Institute of Neuroscience, National Center of Neurology and Psychiatry, Tokyo 187-8502, Japan; †Department of Neurology and Stroke Medicine, Yokohama City University Graduate School of Medicine, Yokohama 236-0004, Japan; ‡Department of Neurology, National Center Hospital, National Center of Neurology and Psychiatry, Tokyo 187-8551, Japan; and §Multiple Sclerosis Center, National Center Hospital, National Center of Neurology and Psychiatry, Tokyo 187-8551, Japan

[1]W.S. and A.T. contributed equally to this work.

[2]Current address: Department of Neurology and Stroke Medicine, Yokohama City University Graduate School of Medicine, Yokohama, Japan.

Received for publication July 23, 2012. Accepted for publication September 11, 2012.

This work was supported by a Research Grant on Super Special Consortia for Supporting the Development of Cutting-Edge Medical Care from Cabinet Office, Government of Japan; a Grant-in-Aid for Scientific Research (S) from the Japan Society for the Promotion of Science (18189009 to T.Y.); and Research Grants on Psychiatric and Neurological Diseases and Mental Health and a Health and Labor Sciences Research Grant on Intractable Diseases (Neuroimmunological Diseases) from the Ministry of Health, Labor and Welfare of Japan.

Address correspondence and reprint requests to Dr. Takashi Yamamura and Dr. Toshimasa Aranami, Department of Immunology, National Institute of Neuroscience, National Center of Neurology and Psychiatry, 4-1-1 Ogawa-Higashi, Kodaira, Tokyo 187-8502, Japan. E-mail addresses: yamamura@ncnp.go.jp (T.Y.) and aranami@ncnp.go.jp (T.A.)

The online version of this article contains supplemental material.

Abbreviations used in this article: BBB, blood–brain barrier; CIS, clinically isolated syndrome; CSF, cerebrospinal fluid; EAE, experimental autoimmune encephalomyelitis; ECD, energy-coupled dye; HS, healthy subject; MBP, myelin basic protein; MMP, matrix metalloproteinase; MS, multiple sclerosis; NHA, normal human astrocyte; NIND, noninflammatory neurologic disease; OIND, other inflammatory neurologic disease; OPN, osteopontin; PB, peripheral blood; RR-MS, relapsing-remitting multiple sclerosis.

Freely available online through *The Journal of Immunology* Author Choice option.

www.jimmunol.org/cgi/doi/10.4049/jimmunol.1202026

IFN-γ worsened MS in a previous clinical trial (13), the role of Th1 cells in MS needs to be analyzed further. In addition, increasing evidence suggest a pathogenic role for cytotoxic effector T cells in MS (14, 15). Moreover, a recent clinical trial of anti–IL-12p40 Ab to block IL-12/IL-23 signaling failed to modulate MS (16), making it difficult to portray a complete picture of MS (9).

Chemokines are a family of secreted proteins that function as key regulators of cell migration via interaction with a subset of seven-transmembrane, G protein-coupled receptors (17, 18). Chemokines are known to be highly efficient and potent chemoattractants for inflammatory cells in EAE (19). In the Th cell-differentiation process, $CD4^+$ T cells acquire the ability to produce sets of cytokines and to express chemokine receptors. Although Th1 cells preferentially express CCR5 and CXCR3, Th2 cells express CCR4 and CRTh2 (20, 21). The chemokine receptor expression pattern would confer to each Th subset a unique characteristic of migration to corresponding ligand chemokines (22). It was recently reported that human Th17 cells are enriched in $CCR4^+CCR6^+$, $CCR2^+CCR5^-$, and $CCR6^+$ populations (23–25).

The present study using multicolor flow cytometry was initiated to address whether Th17 cells bearing Th17 phenotypes ($CCR4^+$ $CCR6^+$, $CCR2^+CCR5^-$, or $CCR6^+$) are increased in the CSF of patients with MS compared with the peripheral blood (PB). In contrast to our expectations, none of these populations was increased in the CSF of MS. Instead, we found that T cells expressing both CCR2 and CCR5 were selectively enriched in the CSF of patients with exacerbated MS but not in patients with other neurologic diseases. The $CCR2^+CCR5^+$ memory $CD4^+$ T cells were shown to produce IFN-γ (24). Comparison with other memory T cell subpopulations revealed that the $CCR2^+CCR5^+$ T cells possessed a distinct ability to produce MMP-9 and OPN, which are critical for initiating and perpetuating the inflammatory pathology in the CNS (4, 7). Consistent with the increased production of MMP-9, which is capable of degrading basement membranes, the $CCR2^+$ $CCR5^+$ T cells showed a greater potential to invade across an in vitro model of the glia limitans, the physiological barrier separating CSF from the CNS parenchyma. Furthermore, the $CCR2^+CCR5^+$ T cells in the PB of active MS contained MBP-reactive T cells producing IFN-γ. We further demonstrated that $CCR6^-$, but not $CCR6^+$, cells within $CCR2^+CCR5^+$ T cells were enriched in the CSF of patients with MS during relapse and expressed high levels of IFN-γ and MMP-9. These results suggest that $CCR2^+CCR5^+CCR6^-$ Th1 cells play a crucial role in the pathogenesis of MS.

Materials and Methods

Subjects

Thirty-four RR-MS patients were examined for the expression of chemokine receptors on T cells. As controls for MS, 11 sex- and age-matched healthy subjects (HS), 6 patients with noninflammatory neurologic disease (NIND), and 4 patients with other inflammatory neurologic disease (OIND) were enrolled in this study. All of the MS patients fulfilled the diagnostic criteria of McDonald et al. (26). Patients with serum aquaporin 4 Abs or with longitudinally extensive spinal cord lesions on the magnetic resonance imaging scan were excluded from this study. In this article, we define "MS in remission" as patients who have been clinically stable without i.v. corticosteroid pulse therapy for >1 mo; "MS in relapse" is defined as patients who have developed an apparent exacerbation within an interval of 1 wk. The detailed demographic characteristics of the cohorts are summarized in Table I. None of the above patients had received IFN-β, i.v. corticosteroids, other immunomodulatory drugs, plasma exchange, or i.v. Ig for ≥1 mo before blood sampling.

CSF and PB pairs were obtained from 12 MS patients in relapse, 6 NIND patients, and 4 OIND patients (Table I). Although NIND patients were significantly older than the MS patient cohort, we confirmed that there was no correlation between age and the frequency of T cell subsets in the CSF of NIND patients. All MS patients were recruited from the National Center Hospital, National Center of Neurology and Psychiatry. OIND patients were recruited from the Yokohama City University Graduate School of Medicine. Written informed consent was obtained from all of the subjects. The National Center of Neurology and Psychiatry Ethics Committee approved this study.

Reagents

Anti–CCR2-biotin, anti–CCR5-FITC, anti–CCR6-FITC, and anti–CCR7-FITC mAb were purchased from R&D Systems (Minneapolis, MN). Streptavidin-PE, streptavidin–energy-coupled dye (ECD), anti–CD45RA-ECD, and mouse IgG1-FITC mAb were purchased from Beckman Coulter (Brea, CA). Anti–CD4-PerCP-Cy5.5, anti–CCR4-PE-Cy7, anti–CCR5-allophycocyanin, anti–CCR4-PE, and anti–CCR6-biotin mAb were purchased from BD Biosciences (San Jose, CA). Human MBP was prepared as described previously (27). For cell culture medium, we used RPMI 1640 (Invitrogen, La Jolla, CA) supplemented with 0.05 mM 2-ME, 2 mM L-glutamine, 100 U/ml penicillin/streptomycin, and 10% FBS.

Cell preparation

PBMC were freshly isolated by density-gradient centrifugation using Ficoll-Paque Plus (GE Healthcare, Oakville, ON, Canada). We used a Memory $CD4^+$ T cell isolation kit (Miltenyi Biotec, Bergisch Gladbach, Germany) to purify memory $CD4^+$ T cells from PBMC. Briefly, PBMC were labeled with a mixture of biotin-conjugated mAb directed against nonmemory $CD4^+$ T cells and then reacted with magnetic microbead-conjugated anti-biotin mAb. The magnetically labeled nonmemory $CD4^+$ T cells were depleted with auto-MACS (Miltenyi Biotec), which yielded >80% purity of memory $CD4^+$ T cells, as assessed by flow cytometry.

To further separate memory $CD4^+$ T cells according to CCR2, CCR5, CCR4, and CCR6 expression, the cells were labeled with anti–CCR2-biotin, anti–CCR5-allophycocyanin, anti–CCR4-PE-Cy7, and anti–CCR6-FITC mAb and streptavidin-PE, in addition to CD4-PerCP-Cy5.5 and CD45RA-ECD. The stained cells were separated by a flow cytometric cell sorter (FACSAria; BD Biosciences). To measure Ag-specific responses, memory $CD4^+$ T cells were separated into $CCR2^+CCR5^+$ T cells and those depleted of $CCR2^+CCR5^+$ T cells by the cell sorter FACSAria II (BD Biosciences). To prepare APC, PBMC depleted of memory $CD4^+$ T cells were stained with anti–CD3-allophycocyanin-Cy7 and anti–CD56-PE mAb. Subsequently, $CD3^-CD56^-$ cells were sorted by FACSAria II and used as APC. This procedure yielded >95% purity of the cells.

Flow cytometric analysis of chemokine receptors

To evaluate expression of chemokine receptors on memory $CD4^+$ T cells, PBMC were first labeled with magnetic microbead-conjugated anti-CD14 mAb, and the labeled $CD14^+$ cells were depleted with auto-MACS, which yielded >95% purity of non-$CD14^+$ PBMC. $CD14^+$ cell-depleted PBMC were stained with anti–CD4-PerCP-Cy5.5, anti–CD45RA-ECD, anti–CCR2-biotin, anti–CCR5-allophycocyanin, anti–CCR4-PE-Cy7, and anti–CCR6-FITC mAb, as well as streptavidin-PE. anti–CCR7-FITC, anti–CCR4-PE, and anti–CCR6-biotin mAb and streptavidin-ECD were used for the staining of CCR7. CSF cells were stained directly with the above-mentioned Abs without depleting $CD14^+$ cells. An isotype control of each Ab was used as a negative control. At the end of the incubation, cells were washed and resuspended in PBS supplemented with 0.5% BSA and immediately analyzed by FACSAria.

Cell culture and cytokine measurements by ELISA

Purified memory $CD4^+$ T cell subsets were suspended at 5×10^5 cells/ml and stimulated with PMA (50 ng/ml) and ionomycin (500 ng/ml) in 96-well U-bottom plates for 24 h. The concentrations of IFN-γ, IL-17, and OPN in the supernatants were measured by Human IFN-γ ELISA Set (BD Biosciences), Human IL-17 DuoSet (R&D Systems), and Human Osteopontin DuoSet (R&D Systems). The procedures were performed according to the manufacturers' instructions.

Intracellular cytokine staining of IL-17 and IFN-γ

Purified memory $CD4^+CCR2^+CCR5^+$ and $CD4^+CCR2^-CCR5^+$ T cells were stimulated with PMA and ionomycin in the presence of monensin for 18 h, fixed in PBS containing 2% paraformaldehyde, and permeabilized with 0.1% saponin. Subsequently, the cells were stained with anti–IL-17-Alexa Fluor 488 and anti–IFN-γ-PE-Cy7 mAb (eBioscience, San Diego, CA). Mouse IgG1-Alexa Fluor 488 and Mouse IgG1-PE-Cy7 were used as isotype control Abs.

T cell stimulation with MBP

To assess the presence of memory MBP-reactive T cells in the purified T cell subsets, FACS-sorted T cell subsets (2×10^4 cells/well) were cocultured

with the irradiated (3500 rad) APC (2×10^5 cells/well), in the presence or absence of MBP (10 μg/ml) or OVA (10 μg/ml), in 96-well flat-bottom plates for 5 d. rIL-2 (20 IU/ml) was added to support the growth of T cells. Cytokine concentrations in the culture supernatants were measured by ELISA.

Real-time RT-PCR

FACS-sorted cells were stimulated with PMA and ionomycin for 12 h, as described above. Total RNA was extracted from cultured cells with an RNeasy Mini Kit (QIAGEN, Tokyo, Japan), according to the manufacturer's instructions. cDNA was synthesized with a PrimeScript RT-PCR kit using oligo-dT Primers (Takara Bio, Otsu, Shiga, Japan). Gene expression was quantified by LightCycler (Roche Diagnostics, Indianapolis, IN) with SYBR Premix Ex Taq (Takara Bio). All procedures were performed according to the manufacturers' protocols. mRNA levels were normalized to endogenous β-actin (ACTB) in each sample. The specific primers used in this study are listed in Table III.

Zymography

MMP-9 activity was determined as previously reported (28). Briefly, SDS-polyacrylamide gels were copolymerized with 1 mg/ml type A gelatin derived from porcine skin (Sigma-Aldrich, St. Louis, MO). $CCR2^+CCR5^+$ T cells and $CD4^+$ T cells depleted of $CCR2^+CCR5^+$ T cells were stimulated with PMA and ionomycin, and 20 μl the culture supernatant and recombinant MMP-9 were electrophoresed. The gels were washed twice in 2% Triton X-100 for 30 min and incubated for 18 h at 37°C in buffer (150 mM NaCl, 50 mM Tris-HCl, 5 mM $CaCl_2$, and 0.02% NaN_3, [pH 7.5]). After fixing with methanol containing acetic acid, the gels were stained with 0.1% Coomassie blue R-250 (Nakarai Tesque, Kyoto, Japan). The gels were scanned with a UV transilluminator (BioDoc-It Imaging System, UVP, Upland, CA) in grayscale mode, and the image was inverted by Adobe Photoshop (Adobe Systems, Mountain View, CA). Recombinant MMP-9 (GE Healthcare) was used as a positive control.

Migration assay

Migration assays were performed with 24-well Transwell membrane inserts (Corning, Wilkes-Barre, PA). The upper sides of Transwell membrane inserts (8 μm; Corning) were coated with 10 μg/ml laminin-1 (Sigma) or 20 μg/ml laminin-2 (Bio Lamina, Stockholm, Sweden). After aspirating the laminin solutions, the membrane inserts were turned upside down, and normal human astrocytes (NHA; Takara Bio) were seeded on the lower sides of the membrane inserts (2×10^5/well). After 18 h, astrocytes formed a confluent monolayer, as confirmed by Diff-Quick staining. Then the membranes were washed twice with RPMI 1640 medium supplemented with 10% FBS and settled in a 24-well plate. PBMC from HS were sorted into memory $CD4^+CCR2^+CCR5^+$ T cells, memory $CD4^+$ T cells depleted of $CCR2^+CCR5^+$ T cells, and memory $CD4^+$ T cells by flow cytometry. These T cells were stimulated with plate-bound anti-CD3/CD28 mAb for 60 h. Then the cells were harvested, suspended in the fresh medium, and seeded onto the upper chambers at 1×10^5 cells/ well, and 600 μl the medium was added to the lower chambers. After 8 h, 500 μl cell suspension was collected from the lower chambers after careful pipetting, and absolute numbers of migrated cells were counted by flow cytometry using Trucount tubes (BD Bioscience).

Statistics

A one-way ANOVA test was used to compare the frequency of chemokine receptor expression within each group of patients or HS. A paired Student *t* test was used to evaluate the difference in the percentage inhibition of migration and in the frequency of chemokine receptor expression between PB and CSF from the same patients. For statistical analysis of other data, an unpaired Student *t* test or one-way ANOVA was used. The p values < 0.05 were considered statistically significant.

Results

$CCR2^+CCR5^+$ T cells are enriched in the CSF of MS patients in relapse

First, we analyzed the chemokine receptor-expression profile of memory $CD4^+$ T cells in the PB of MS patients (Table I) compared with HS and those with NIND. Multicolor flow cytometric analysis was performed on PBMC after staining with differentially labeled anti-CCR2, -CCR4, -CCR5, and -CCR6 mAb. Patterns of coexpression for four chemokine receptors are summarized in Supplemental Fig. 1 and Supplemental Table I. When the memory T cells in PB were grouped based on CCR2 versus CCR5 or CCR4 versus CCR6 expression (Fig. 1A), no particular population was found to be altered in MS patients compared with HS or NIND patients, irrespective of whether the MS patients were in relapse or in remission (Fig. 1B). We next analyzed sets of CSF and PB samples from individual patients with MS, OIND, or NIND. As shown in Fig. 1C, $CCR2^-CCR5^+$ T cells formed the predominant T cell population in the CSF of patients with NIND or MS during relapse, suggesting that this population, which was previously shown to be enriched for Th1 cells (24), is allowed to enter the CSF spaces in the patients with MS and NIND. It was reported that human IL-17–producing T cells or Th17 cells are enriched in $CCR2^+CCR5^-$, $CCR4^+CCR6^+$, or $CCR6^+$ cells (23–25). We were initially interested in knowing whether examination of the chemokine receptor profile could reveal an increase in Th17 cells in the CSF of MS patients. However, the frequencies of $CCR2^+CCR5^-$, $CCR4^+CCR6^+$, and $CCR6^+$ cells were lower, rather than higher, in the CSF compared with the PB of patients with MS or NIND. In contrast, the frequency of $CCR2^+CCR5^+$ T cells in the CSF of patients with MS was significantly higher than in the PB (Fig. 1C). Of note, this increase was specific for MS and was not found in the patients with other neurologic diseases, indicating that cells of this subset are selectively recruited to autoimmune inflammatory lesions or would expand in the CSF during relapse of MS. In addition, if we separate the MS patients by disease duration (<10 y [$n = 8$] or >10 y [$n = 4$]), the higher frequency of $CCR2^+CCR5^+$ T cells in CSF compared with PB was evident ($p < 0.0005$) in those with the shorter history of MS (<10 y) (Fig. 2, Table II), but not in those with longer history (data not shown). We also noted that enrichment for $CCR2^-CCR5^+$ T cells in the CSF was not detected in the patients with the shorter history of MS. In contrast, the proportion of $CCR4^+CCR6^+$ T cells was significantly lower ($p < 0.005$) in CSF compared with PB of these

Table I. Patient summary

PB Analysis	MS in Remission	MS in Relapse	HS	NIND[a]
Males/females (*n*)	3/8	5/6	5/6	2/4
Age (y; mean ± SD)	44 ± 12	42 ± 13	39 ± 5	64 ± 13
PB/CSF Analysis	**MS in Relapse[b]**	**NIND**	**OIND[c]**	
Males/females (*n*)	5/7	2/4	2/2	
Age (y; mean ± SD)	46 ± 15	64 ± 13	44 ± 14	

[a]NIND includes one patient with Parkinson's disease, one patients with myasthenia gravis, three patients with normal pressure hydrocephalus, and one patient with multiple system atrophy.

[b]Five MS patients were being treated with immunomodulatory drugs (one with IFN-β, two with oral corticosteroids, and two with an immunosuppressive drug) before their relapses.

[c]OIND includes one patient with mumps meningitis, one patient with herpes encephalitis, and two patients with undiagnosed viral meningitis in acute phase.

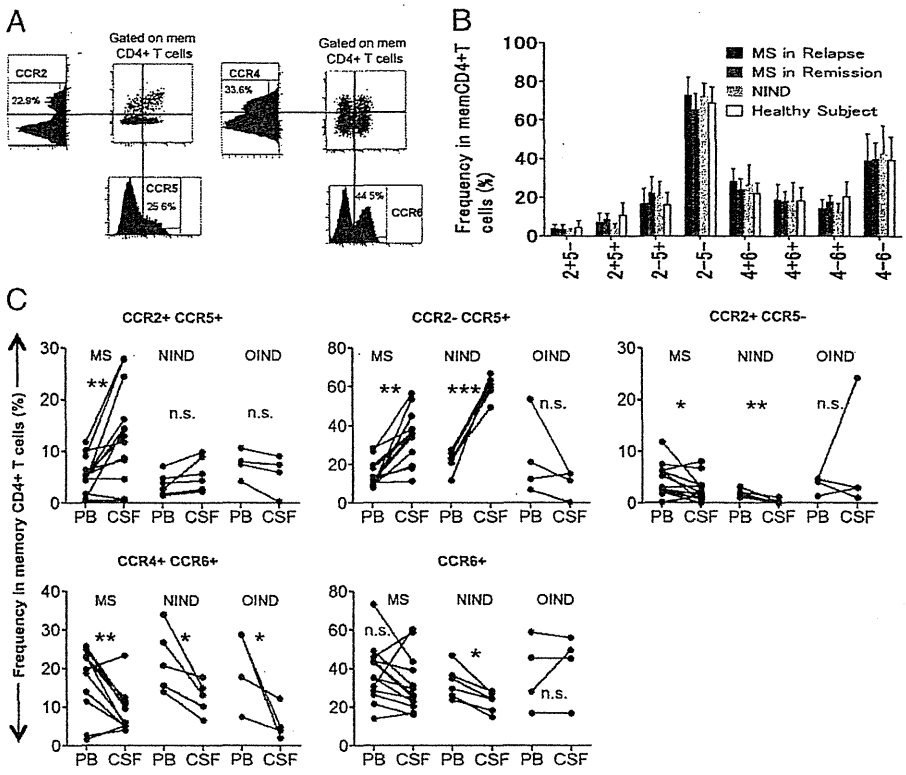

FIGURE 1. CCR2$^+$CCR5$^+$ T cells are enriched in the CSF of MS patients in relapse. (**A**) PBMC depleted of CD14$^+$ cells were stained with differentially labeled anti-CD4, -CD45RA, -CCR2, -CCR5, -CCR4, and -CCR6 mAb simultaneously. The CD4$^+$CD45RA$^-$ population was analyzed for expression of CCR2 and CCR5 (*left panels*) or CCR4 and CCR6 (*right panels*). Graphs of the corresponding parameters are also shown. Numbers (%) indicate the percentage of the positive population in the graphs. (**B**) Cells were stained, as described in (A), and frequencies of T cell subsets in memory CD4$^+$ T cells of 11 MS patients in relapse, 11 MS patients in remission, 6 NIND patients, and 11 HS were calculated. For brevity, "CCR" is omitted from the figure (e.g., 2+5− represents CCR2$^+$CCR5$^-$). (**C**) Comparison of the frequencies of the T cell subsets in the CSF and PB from 12 MS patients in relapse, 6 patients with NIND, and 4 patients with OIND. Lines connect data for paired CSF and PB samples from the same patients. $*p < 0.05$, $**p < 0.005$, $***p < 0.0005$. n.s., Not significant.

MS patients. These results indicate that selective enrichment of CCR2$^+$CCR5$^+$ T cells in the CSF is detected in relatively early stages of MS.

CCR2$^+$CCR5$^+$ T cells in the PB contain both central and effector memory cells and produce both IFN-γ and IL-17

Memory CD4$^+$ T cells are divided into CCR7$^+$ central memory and CCR7$^-$ effector memory subsets, which are differentially endowed with effector functions (29). The staining of CCR7, together with CCR2/5 or CCR4/6, revealed a higher effector memory/central memory ratio in CCR2$^+$CCR5$^+$ T cells and CCR2$^-$CCR5$^+$ T cells (Supplemental Fig. 2). We next analyzed cytokine production by each T cell population bearing a distinct chemokine receptor profile. The cells of interest were separated from PB of HS and were stimulated with PMA and ionomycin. Compared with unfractionated memory CD4$^+$ T cells, CCR2$^+$CCR5$^+$ and CCR2$^-$CCR5$^+$ T cells produced a larger quantity of IFN-γ (Fig. 3A). Although CCR2$^+$CCR5$^+$ T cells produced a significant amount of IL-17, production of IL-17 from CCR2$^-$CCR5$^+$ T cells was only marginal. CCR2$^+$CCR5$^-$ T cells and CCR4$^+$CCR6$^+$ T cells selectively produced IL-17, whereas CCR4$^-$CCR6$^-$ T cells selectively produced IFN-γ. These results were consistent with the results of previous studies (23, 24). Because T cells expressing both IFN-γ and IL-17 are reportedly present in highly infiltrated lesions of MS brain sections (12), it was of interest to know whether similar T cells producing both IFN-γ and IL-17 are present in CCR2$^+$CCR5$^+$ T cells. By conducting intracellular cytokine staining, we revealed that the CCR2$^+$CCR5$^+$ T cells, as well as CCR2$^-$CCR5$^+$ T cells, are composed of IFN-γ$^+$IL-17$^-$ cells, IFN-γ$^+$IL-17$^+$ cells,

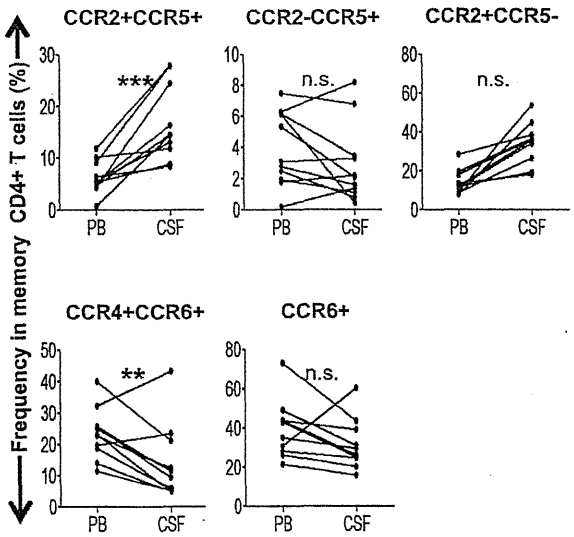

FIGURE 2. Frequencies of the T cell subsets in the CSF and PB from eight MS patients with disease duration <10 y. $**p < 0.005$, $***p < 0.0005$. n.s., Not significant.

Table II. CCR2$^+$CCR5$^+$ T cells are involved in early stages of MS

Clinical Parameter	Disease History <10 y	Disease History >10 y
Disease duration (y; mean ± SD)	4.8 ± 3.8	15.5 ± 4.4
No. of patients	8[a]	4[b]
Age (y; mean ± SD)	42 ± 14	54 ± 15
Relapse rate (times/y; mean ± SD)	1.8 ± 0.9	2.0 ± 14
EDSS (mean ± SD)	3.1 ± 0.7	4.0 ± 1.2
No. of patients with more CCR2$^+$CCR5$^+$ T cells in CSF than in PB	8*	0

[a]Three patients were treated with IFN-β ($n = 1$), oral steroid ($n = 1$), or immunosuppressant ($n = 1$).
[b]Two patients were treated with oral steroid.
$*p < 0.0005$.

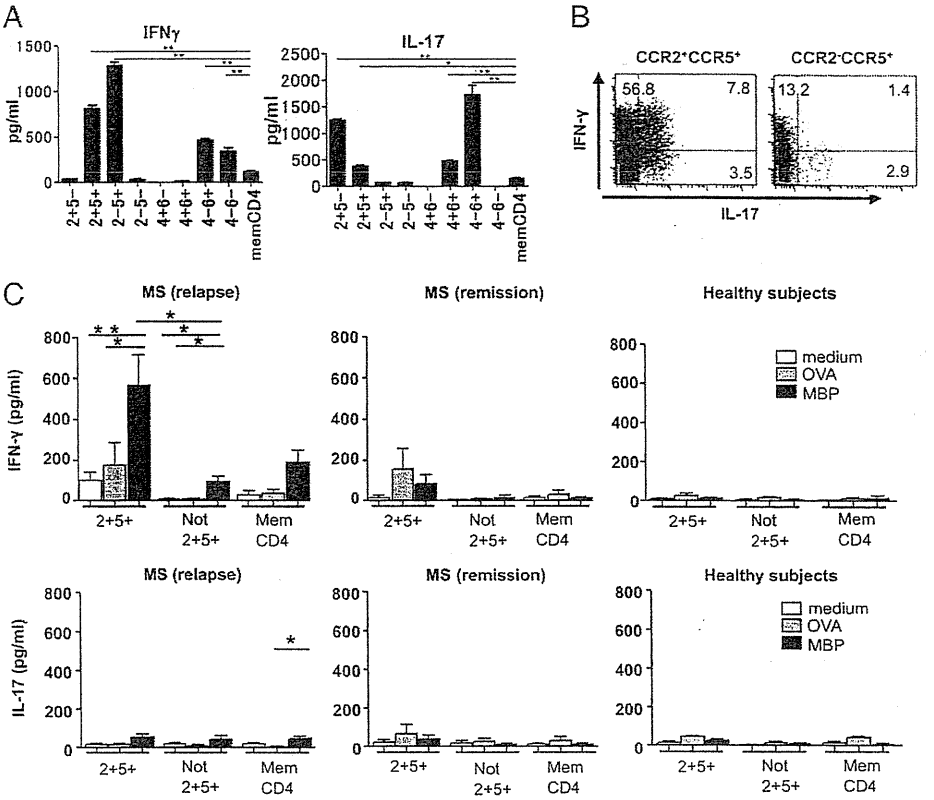

FIGURE 3. Cytokine production and reactivity to MBP by $CCR2^+CCR5^+$ T cells in the PB. (**A**) Memory $CD4^+$ T cell subsets purified from PBMC of HS by flow cytometry were stimulated with PMA and ionomycin. Concentrations of IFN-γ and IL-17 in the supernatants were measured by ELISA. Data represent mean ± SD of three HS. (**B**) Purified $CCR2^+CCR5^+$ T cells (*left panel*) and $CCR2^-CCR5^+$ T cells (*right panel*) were stimulated with PMA and ionomycin for 18 h, and the production of IL-17 and IFN-γ was assessed by intracellular cytokine staining. Numbers indicate the frequency (%) of cells in each quadrant. One representative experiment from three independent experiments with PBMC from HS is shown. (**C**) Purified memory $CD4^+$ T cell subsets were cultured in duplicate with irradiated APC in the presence of MBP (10 μg/ml) or OVA (100 μg/ml) for 5 d. Concentrations of IFN-γ and IL-17 in the supernatants were measured by ELISA. Data represent mean ± SD of six MS patients in relapse, three MS patients in remission, and three HS. $*p < 0.05$, $**p < 0.005$.

and IFN-γ^-IL-17^+ cells (Fig. 3B). In both T cell populations, IFN-γ^+IL-17^- cells were a major subset of IFN-γ production.

$CCR2^+CCR5^+$ T cells in the PB from MS patients during relapse are reactive to MBP

Given that the $CCR2^+CCR5^+$ T cells are proportionally higher in CSF than PB of MS during relapse, we were interested to know whether the $CCR2^+CCR5^+$ T cells are enriched in autoimmune, pathogenic T cells. We therefore examined if the $CCR2^+CCR5^+$ T cells might react to MBP, a putative autoantigen for MS. We isolated memory $CD4^+CCR2^+CCR5^+$ T cells and memory $CD4^+$ T cells depleted of $CCR2^+CCR5^+$ T cells from the PB of MS in relapse, MS in remission and HS. We stimulated these cells with MBP or OVA in the presence of autologous APC and measured the levels of IFN-γ and IL-17 in the supernatants after culture (Fig. 3C). The T cell populations separated from HS did not show any significant response to MBP or OVA in this assay. A marginal IFN-γ response to MBP and OVA was noted in $CCR2^+CCR5^+$ T cells from MS in remission. Strikingly, the $CCR2^+CCR5^+$ T cells from MS in relapse selectively and significantly responded to MBP by producing a large amount of IFN-γ, whereas those depleted of $CCR2^+CCR5^+$ T cells or total memory $CD4^+$ T cells showed a much smaller response. These results suggest that MBP-specific IFN-γ-producing cells might be enriched in $CCR2^+$ $CCR5^+$ T cells during relapse of MS.

$CCR2^+CCR5^+$ T cells in the PB produce MMP-9 and OPN

Lymphocyte migration/infiltration is a critical step for the development of autoimmune pathology in the CNS, and two physical barriers protect the CNS parenchyma from entry of the immune cells: the vascular endothelium barrier and the glia limitans barrier made up of extending astrocyte foot processes (8, 30). Each barrier possesses its own basement membrane, and the CSF circulates in the perivascular space between the two membranes. Thus, initiation of CNS inflammation requires immune cells that are capable of disrupting these physical barriers. Because type IV collagenase MMP-9 is selectively elevated in the CSF in MS, MMP-9 is assumed to play a role in disrupting the BBB in MS (28, 31, 32). Speculating that $CCR2^+CCR5^+$ T cells may have a distinct ability to initiate the processes of CNS inflammation, we examined whether $CCR2^+CCR5^+$ T cells are able to produce MMP-9. Strikingly, quantitative RT-PCR analysis of whole and CCR2/CCR5 fractions of memory T cells from HS and MS showed that expression of MMP-9 was mainly restricted to $CCR2^+CCR5^+$ T cells (Fig. 4A, 4B, Table III). The expression of MMP-1 and MMP-19, which also possess the potential to degrade the basement membrane, was highest in $CCR2^+CCR5^+$ T cells, whereas all T cell populations similarly expressed MMP-10 and MMP-28 (Supplemental Fig. 3). We also measured MMP-2, -7, -14, -15, -23, and -25, but none of these was detected. Using zymography, we further examined MMP-9 enzymatic activity in the culture supernatants of activated $CCR2^+CCR5^+$ T cells. As shown in Fig. 4C, supernatants from $CCR2^+CCR5^+$ T cells exhibited MMP-9 activity, but those from T cells depleted of the $CCR2^+CCR5^+$ population did not.

Recent studies suggested that OPN, which is also expressed by T cells (33, 34), might be involved in the pathogenesis of MS. Although OPN-deficient mice were resistant to relapse of EAE (4, 33), administration of recombinant OPN to OPN-deficient mice reversed the ongoing remission of the disease and induced progressive exacerbation of the clinical symptoms (4). These findings prompted us to examine whether OPN is overexpressed in $CCR2^+$ $CCR5^+$ T cells after stimulation with PMA and ionomycin. As shown in Fig. 4D and 4E, $CCR2^+CCR5^+$ T cells expressed a much higher level of OPN than did the other memory T cell populations at both the mRNA and the protein levels.